NACA

RESEARCH MEMORANDUM

LOW-SPEED WIND-TUNNEL INVESTIGATION OF THE LONGITUDINAL STABILITY CHARACTERISTICS OF A MODEL EQUIPPED WITH A VARIABLE-SWEEP WING

By

Charles J. Donlan and William C. Sleeman, Jr.

Langley Aeronautical Laboratory
Langley Air Force Base, Va.

NATIONAL ADVISORY COMMITTEE
FOR AERONAUTICS

WASHINGTON

May 23, 1949

NATIONAL ADVISORY COMMITTEE FOR AERONAUTICS

RESEARCH MEMORANDUM

LOW-SPEED WIND-TUNNEL INVESTIGATION OF THE LONGITUDINAL STABILITY CHARACTERISTICS OF A MODEL EQUIPPED WITH A VARIABLE-SWEEP WING

By Charles J. Donlan and William C. Sleeman, Jr.

SUMMARY

An investigation has been made to determine the longitudinal stability characteristics of a complete model equipped with a variable-sweep wing at angles of sweepback of 45°, 30°, 15°, and 0°. The investigation was directed toward the study of various wing modifications and an external-flap arrangement designed to minimize the shift in neutral point accompanying the change in sweep angle.

The results indicated that stability at the stall was obtained at a sweep angle of 15° without recourse to stall-control devices. The basic neutral-point movement accompanying the change in sweep angle from 45° to 15° amounted to 56 percent of the mean aerodynamic chord (at zero sweep angle) and the most effective modification investigated only reduced this change to 47 percent of the chord. It appears, therefore, that for designs in which the fuselage is the major load-carrying element some relative movement between the wing and center of gravity will be required to assure satisfactory stability at all sweep angles.

INTRODUCTION

The use of swept wings on high-speed airplanes has introduced serious longitudinal- and lateral-stability problems at low speeds. Many high-lift and stall-control devices have been investigated in an attempt to improve the low-speed characteristics of highly swept wings but no completely satisfactory solution has been found. One obvious method for avoiding the low-speed problems associated with highly swept wings would be to employ a wing whose sweep angle could be varied in flight. Thus, for maximum high-speed flight and optimum cruising performance, the wing could be adjusted to any desired sweep angle; whereas, for the landing condition, the sweep angle could be decreased to an angle that would assure satisfactory low-speed characteristics without recourse to stall-control devices.

The present paper presents the results of a wind-tunnel investigation of a complete model equipped with a wing whose sweep angle could be varied for the purpose of studying various wing modifications designed to decrease

the large forward movement of the neutral point that was found in reference 1 to accompany the decrease in sweepback. Much of the basic data is presented in reference 1 but in that paper the pitching-moment coefficients are based on the mean aerodynamic chord associated with each sweep angle and the assumed pitching-moment reference axis was at 25 percent of the mean aerodynamic chord for each sweep angle. In the present paper a common chord and common reference axis were used in computing the pitching-moment coefficients for all sweep angles investigated.

COEFFICIENTS AND SYMBOLS

The results of the tests are presented as standard NACA coefficients of forces and moments. Pitching-moment coefficients are given about the center-of-gravity location shown in figure 1 (25 percent of the mean aerodynamic chord at 0° sweep). The data are referred to the stability axes; the positive directions and angular displacements are shown in figure 2.

The coefficients and symbols are defined as follows:

C_L	lift coefficient (Lift/qS)
C_{L_o}	tail-off lift coefficient
C_X	longitudinal-force coefficient (X/qS)
C_m	pitching-moment coefficient (M/qSc')
q	free-stream dynamic pressure, pounds per square foot ($\rho V^2/2$)
S	wing area without cutout, square feet (varies with angle of sweep)
S_t	horizontal-tail area, square feet
c	airfoil section chord, feet
c'	wing mean aerodynamic chord (1.181 ft for $\Lambda = 0^\circ$)
c_t	wing tip chord measured parallel to plane of symmetry, feet
c_r	wing root chord at plane of symmetry, feet
b	wing span, feet
V	air velocity, feet per second

ρ mass density of air, slugs per cubic foot

α angle of attack of fuselage center line, degrees

Λ angle of sweepback of quarter-chord line of wing, degrees

ϵ downwash angle, degrees

i_t angle of stabilizer with respect to fuselage center line, degrees

λ wing taper ratio (c_t/c_r)

δ_f flap deflection, degrees

n_o tail-off aerodynamic-center location, percent wing mean aerodynamic chord for $\Lambda = 0^\circ$

n_p neutral-point location, percent wing mean aerodynamic chord for $\Lambda = 0^\circ$

MODEL AND APPARATUS

The model used in this investigation (fig. 1) had wing panels which could be rotated about a point on the quarter-chord line to angles of sweepback of 45°, 30°, 15°, and 0°. At 45° sweep the wing tips were parallel to the plane of symmetry. The geometric characteristics of the model are tabulated in table I. The model is shown mounted on a single-support strut in the Langley 300 MPH 7- by 10-foot tunnel in figure 3. Details of the various wing modifications investigated are given in figure 4 and table I. Photographs of the model with the external airfoil flaps installed $(\delta_f = 40^\circ)$ are presented in figure 5.

Structural limitations of the model wing determined the maximum chordwise dimensions of the cutout which was completely enclosed within the fuselage at 45° sweepback.

TESTS

Test Conditions

The tests were made at a dynamic pressure of 30 pounds per square foot, which corresponds to an airspeed of about 108 miles per hour. The test Reynolds number was approximately 1.2×10^6 based on the wing chord of 1.181 feet (c' at $\Lambda = 0^\circ$). The degree of turbulence of the

tunnel is not known, but is believed to be small because of the large contraction ratio (14 to 1).

The aerodynamic coefficients for all configurations were based on the wing area without cutout. All pitching-moment data were based on a chord of 1.181 feet (c' at $\Lambda = 0^\circ$).

Corrections

The data have not been corrected for tares caused by the model-support system inasmuch as, with the arrangement used, the tares are believed to be small. Jet-boundary corrections have been applied to the angles of attack, the drag coefficients, and the tail-on pitching-moment coefficients. The corrections were computed by use of reference 2, which unpublished calculations have indicated to be satisfactory for sweep angles up to 45°.

All forces and moments were corrected for blocking by the method given in reference 3. An increment of longitudinal-force coefficient has been applied to account for the horizontal buoyancy.

RESULTS AND DISCUSSION

The basic aerodynamic characteristics of the model are presented in figures 6 to 9. The longitudinal-stability parameters are presented in figures 10 to 15. For convenient reference, an outline of the summary figures presenting the results is given as follows:

	Figure
Variable sweep:	
(a) Effect of sweep	10
(b) Effect of faired cutout	11, 12, and 13
(c) Effect of vertical location of horizontal tail	12(a), 12(b), 12(c), 12(d), and 14
Modifications to model with 15° sweep:	
(a) Basic tail position	
1. Effect of cutout profile and size	12(a)
2. Effect of flap deflection	12(c)
3. Effect of sharp leading edge	12(e)
4. Effect of wing vane	12(f)
(b) Alternate tail position	
1. Effect of faired cutout	12(c), 12(d)
2. Effect of flap deflection	12(d)
Comparison of basic configuration with most favorable modifications	15

Basic Configurations

Effect of sweep angle, wing without cutouts.— The destabilizing movement of the neutral-point location as the wing sweep angle was decreased amounted to about 2 percent of the chord (c' at $\Lambda = 0^\circ$) per degree change in sweep angle (fig. 10). Inasmuch as the parameters affecting the tail contribution to stability show relatively minor variations with sweep angle, it would appear that the shift in neutral point is primarily associated with the geometric movement of the wing-aerodynamic-center position as the wing is rotated. Up to about 35° of sweep angle the experimental rate of variation of neutral point with sweep angle is in good agreement with that estimated from the simple geometric consideration that the centroid of lift on each wing panel acts at 25 percent of the mean aerodynamic chord of the wing at each sweep angle.

For the 30° and 45° sweep configurations, an unstable variation of pitching-moment coefficient with lift coefficient at the high lift coefficients is indicated (figs. 8 and 9); whereas, for 0° and 15° configurations, stable pitching-moment characteristics were obtained in the vicinity of the maximum lift coefficient.

Effect of sweep angle, wing with faired cutout.— If a cutout is allowed to develop at the juncture of the wing-root trailing edge and the fuselage as the wing sweep angle is decreased (figs. 1 and 4), significant changes in the stability characteristics exhibited by the model can occur. It was anticipated that the cutout would move the wing-aerodynamic-center position forward somewhat but that the downwash field in the vicinity of the horizontal tail would be changed in such a manner that the over-all stability of the model would be increased. The extent to which these effects were manifested at various sweep angles is indicated in figures 11 to 13.

A study of these data indicates that the faired cutout afforded somewhat greater stability than the configurations having no cutout but the over-all effect on stability is small compared to the large changes produced by the geometric movement of the wing aerodynamic center. The effects on the stability parameters were greatest at 0° sweep and decreased as the sweep angle was increased. The tail contribution to stability at sweep angles of 0° and 15° was increased considerably because of favorable flow changes at the tail but this beneficial effect was partially canceled by the forward movement of the wing aerodynamic center caused by the cutouts.

The effect of the faired cutout on the neutral-point position for all sweep angles is summarized in figure 15.

Effect of vertical location of the horizontal tail.— Decreasing the height of the horizontal tail above the wing from the basic position to the alternate position (fig. 1) showed little effect on n_p for the configurations investigated (figs. 12(a), 12(b), and 14). The stability was slightly lower at the higher lift coefficients with the tail in the alternate position owing mainly to a less favorable downwash gradient.

Modifications to Model with 15° Sweepback

Inasmuch as the configuration with 15° sweepback possessed favorable stability characteristics at the stall, this configuration was adopted as the basic low-speed arrangement and various modifications were investigated in an attempt to reduce the large ($0.56c'$) basic shift in neutral point accompanying the reduction in sweep from 45° to 15°.

Effect of cutout profile.— The effects of various cutout arrangements are presented in figure 12(a). From stability considerations, the faired cutout appeared to be superior to the unfaired cutouts and this arrangement was used for the majority of tests with cutouts.

Effect of external airfoil flaps.— In an effort to compensate for the forward movement of the wing aerodynamic center caused by the cutout and at the same time introduce a field of upwash in the vicinity of the cutout, tests were made of a configuration employing essentially full-span external flaps (figs. 4 and 5). The results obtained for the various arrangements tested are presented in figures 7(c), 7(d), 12(c), and 12(d). A comparison of these results with those for the configuration without flaps (figs. 7(a), 7(b), 12(a), and 12(b)) indicate that the flap caused an additional rearward movement of the neutral point of only about $0.02c'$ ($\Lambda = 0°$). The flap arrangement which was used in this investigation was not a particularly effective one, however, as is indicated by the rather low lift and pitching-moment increments produced by the flap. (Compare figs. 7(a) with 7(c).) It is possible that, with a well-designed extensible-slotted-flap arrangement, the rearward neutral-point movement resulting from the deflected flap for the configuration with the wing cutout would be considerably increased.

Sharp leading edge and wing vane.— Several sharp-leading-edge sections and wing vanes mounted on the inboard sections of the wing panel were investigated in an attempt to reduce the lift on this portion of the wing and thereby increase the stability by reducing the downwash gradient. None of these modifications changed the stability characteristics appreciably. Typical results obtained with the sharp leading edge and wing vane are presented in figures 12(e) and 12(f).

Design Considerations

The variation of the static longitudinal stability characteristics with sweepback and model configuration is summarized in figure 15. It is evident that a combination of cutouts and flaps can aid in minimizing the forward neutral-point movement as the sweep angle is decreased to 15° but that translation of the wing is required to compensate for the greater portion of the neutral-point movement. For the sweep range investigated it would be necessary to translate the wing rearward roughly $0.5c'$ ($\Lambda = 0°$) as the sweep angle is decreased to 15° in order to maintain a constant location of the neutral point. It is probable that a sweep angle greater than 15° (but less than 30°) would be satisfactory from low-speed stability considerations. If, for a particular design, the extent of longitudinal wing translation is limited, the maximum sweep angle for which adequate low-speed stability characteristics are attainable should be determined from wind-tunnel experiments.

Although the incorporation of a wing capable of translation as well as rotation affords formidable structural problems, the potential aerodynamic rewards incident to their solution are significant. The ability to adjust the sweep angle in flight not only makes it possible to utilize the most efficient sweep angles for high speed and cruising performance but assures stability in the landing configuration without recourse to wing slots or other stall-control devices. The more efficient moderately swept higher-aspect-ratio wing used for the landing condition can also be equipped with conventional high-lift devices and thus provide minimum landing speeds. The wing sweep angle could be adjusted in flight for optimum cruising configuration, and for the highest sweep angles the wing can be translated to compensate partly for the stability changes usually encountered at the higher Mach numbers with swept wings.

It appears from low-speed stability data that the cutout formed at the wing-fuselage juncture as the wing is rotated forward is beneficial. If high speeds are contemplated with intermediate sweep angles, however, model tests at higher Mach numbers will be required to evaluate the effect of these cutouts.

The amount of wing translation required is also dependent on the mass distribution of the airplane and the location of the wing pivot point. The weight of the wings, the location of wing fuel tanks as well as fuel tanks in other parts of the airplane, and the plan for emptying the fuel tanks in flight must be considered in evaluating the stability of the airplane. In the case of a variable-sweepback flying wing, for example, the center of gravity would move almost as much as the aerodynamic center of the wing. A study of the unlimited configurations that could utilize center-of-gravity movements created by expendable fuel and moving structural elements is, however, beyond the scope of this paper.

CONCLUSIONS

The results of a low-speed wind-tunnel investigation of a complete model having a variable-sweep wing which was tested at 45°, 30°, 15°, and 0° sweepback indicated the following conclusions:

1. Stability at the stall was obtained for the configuration with 15° sweepback without recourse to stall-control devices.

2. The shift in neutral point as the sweep was varied from 45° to 15° was decreased from 56 percent of the chord (c' at $\Lambda = 0°$) in the original case to 47 percent by the most effective combination of the modifications tested.

3. It seems unlikely that satisfactory stability for all flight conditions can be achieved with a variable-sweep wing without recourse to relative translation between the wing and the center of gravity of the airplane.

Langley Aeronautical Laboratory
National Advisory Committee for Aeronautics
Langley Air Force Base, Va.

REFERENCES

1. Spearman, M. Leroy, and Comisarow, Paul: An Investigation of the Low-Speed Static Stability Characteristics of Complete Models Having Sweptback and Sweptforward Wings. NACA RM No. L8H31, 1948.

2. Gillis, Clarence L., Polhamus, Edward C., and Gray, Joseph L., Jr.: Charts for Determining Jet-Boundary Corrections for Complete Models in 7- by 10-Foot Closed Rectangular Wind Tunnels. NACA ARR No. L5G31, 1945.

3. Thom, A.: Blockage Corrections in a Closed High-Speed Tunnel. R. & M. No. 2033, British A.R.C., 1943.

TABLE I

PHYSICAL CHARACTERISTICS OF THE VARIABLE-SWEEP MODEL

Center of gravity, all sweep angles, percent chord (c' at $\Lambda = 0^\circ$) . 25

Wing:

Root and tip sections . . . . . NACA 65_1-110($a = 1.0$)

Incidence (root chord to center line of fuselage), degrees 0

Sweep, Λ (deg)	Area (sq ft)	Span (ft)	c (ft)	Aspect ratio	Taper ratio	Cutout area (sq ft)	
						Faired	Large
0	8.67	8.35	1.181(c')	8.04	0.50	0.24	0.37
15	8.40	7.75	1.181	7.15	.49	.16	.25
30	8.13	6.76	1.181	5.62	.48	.06	.12
45	7.80	5.37	1.181	3.69	.46	----	----

Horizontal tail:

Airfoil section	NACA 65-008
Total area, sq ft	1.625
Span, ft	2.85
Aspect ratio	5.0
Taper ratio	0.50

External airfoil flap:

Airfoil section	23012
Span, percent wing span at $\Lambda = 15^\circ$	64.5
Chord, percent c' ($\Lambda = 0^\circ$)	14.1

NACA

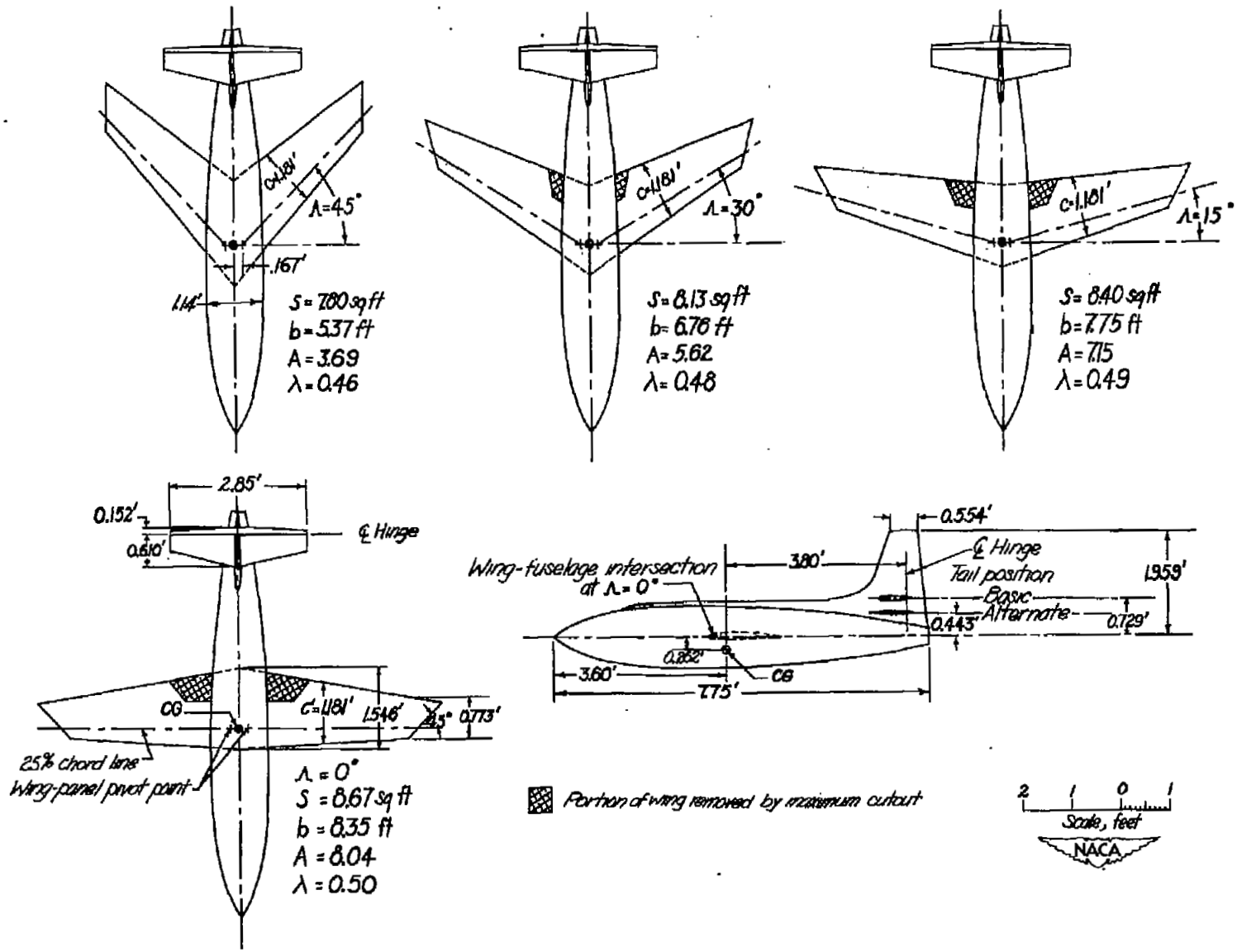

Figure 1.– Drawing of variable-sweep model showing different sweep configurations and horizontal-tail locations.

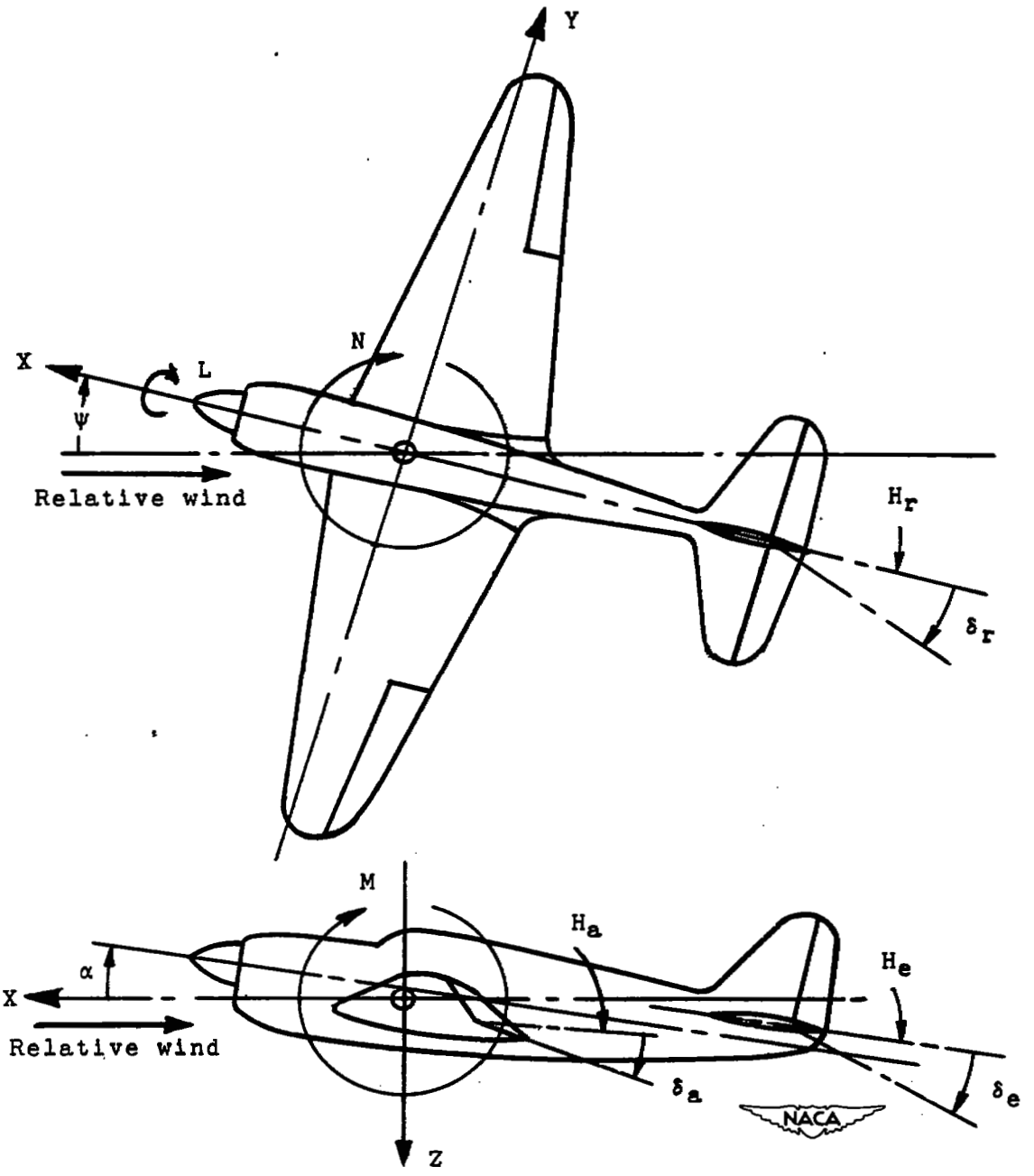

Figure 2.— System of axes and control-surface hinge moments and deflections. Positive values of forces, moments, and angles are indicated by arrows. Positive values of tab hinge moments and deflections are in the same directions as the positive values for the control surfaces to which the tabs are attached.

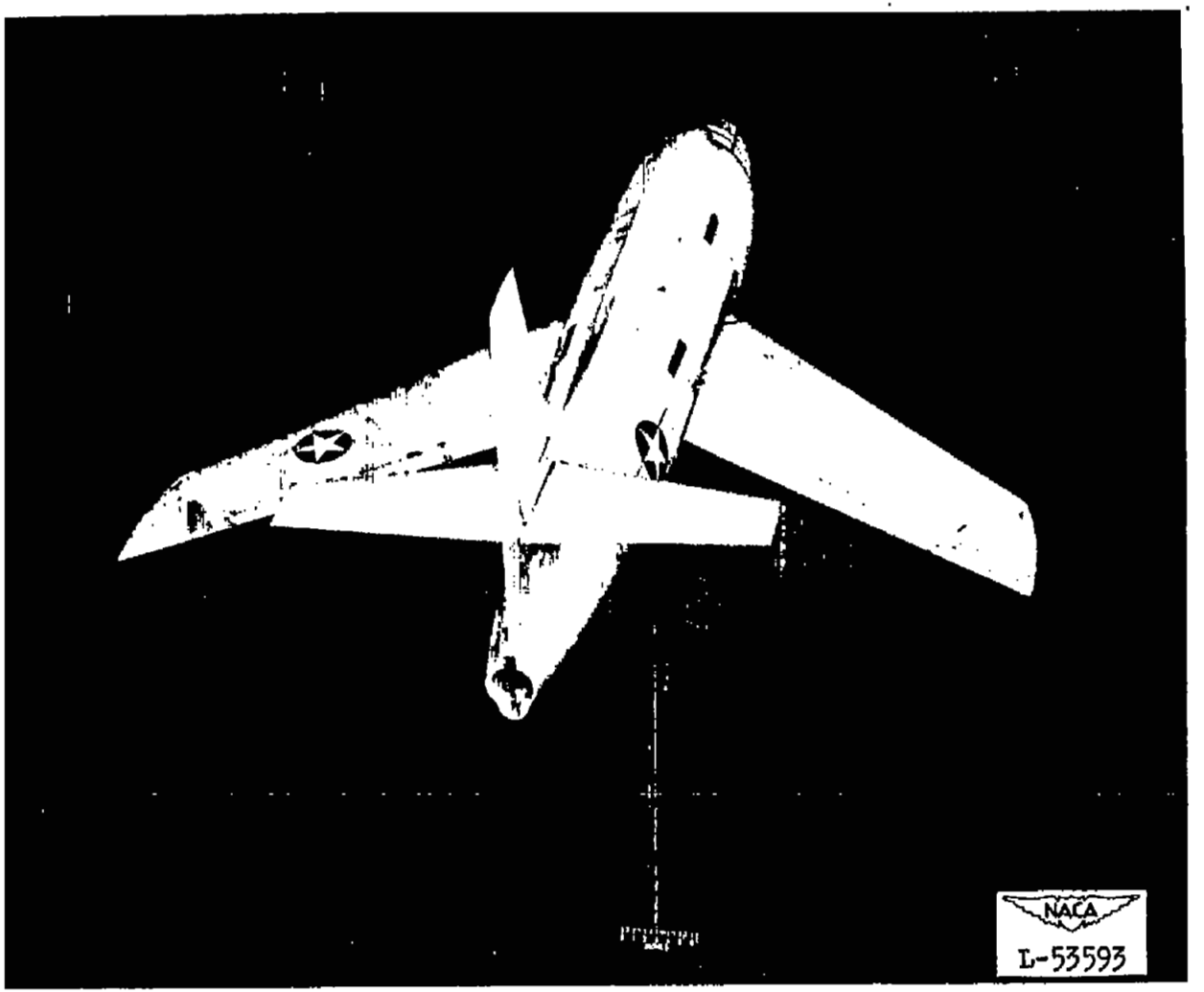

6/47

Figure 3.- Variable-sweep model mounted on single-support strut in 300 MPH 7- by 10-foot tunnel. $\Lambda = 45^{\circ}$; rear view.

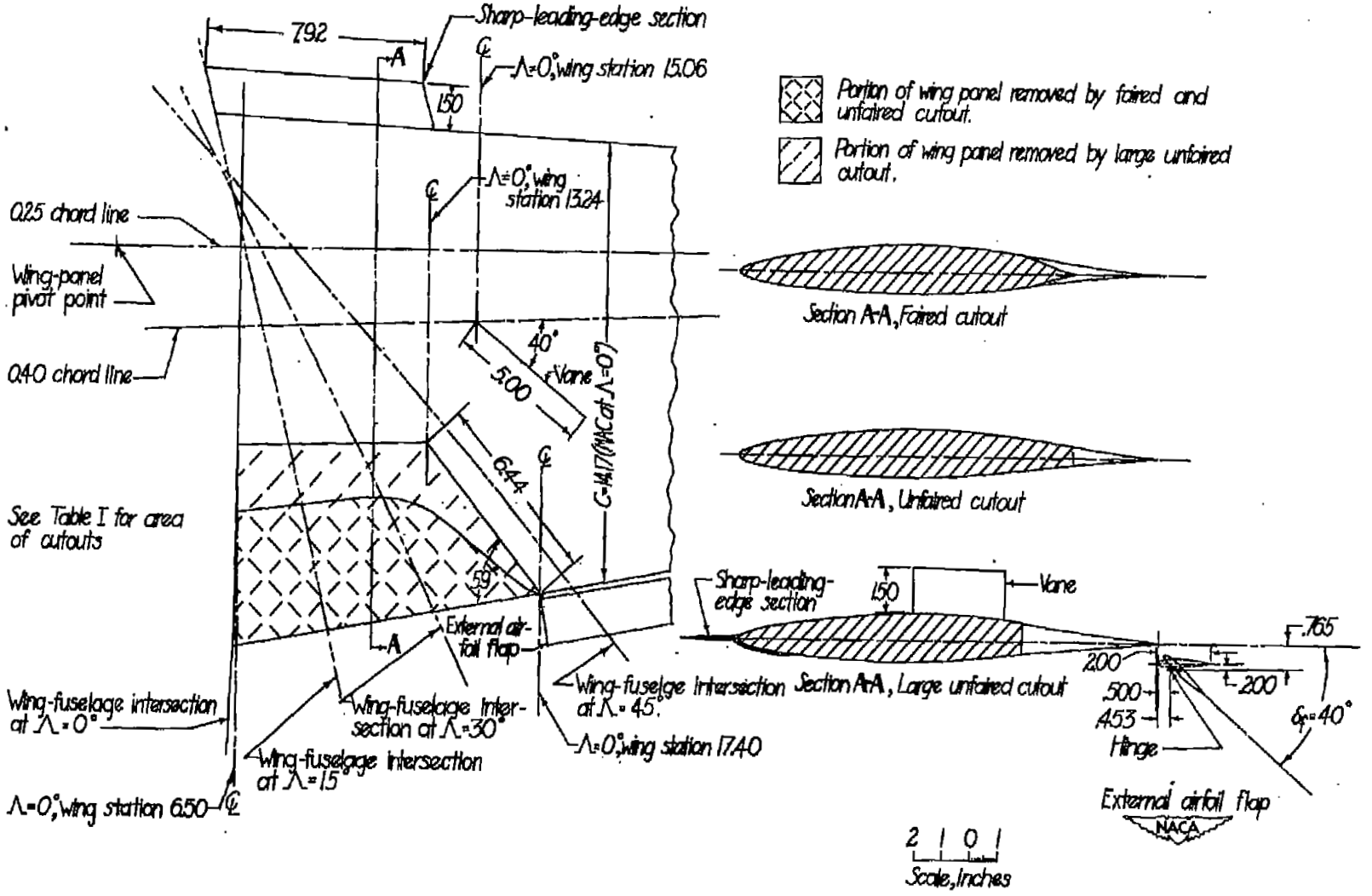

Figure 4.- Details of wing modifications.

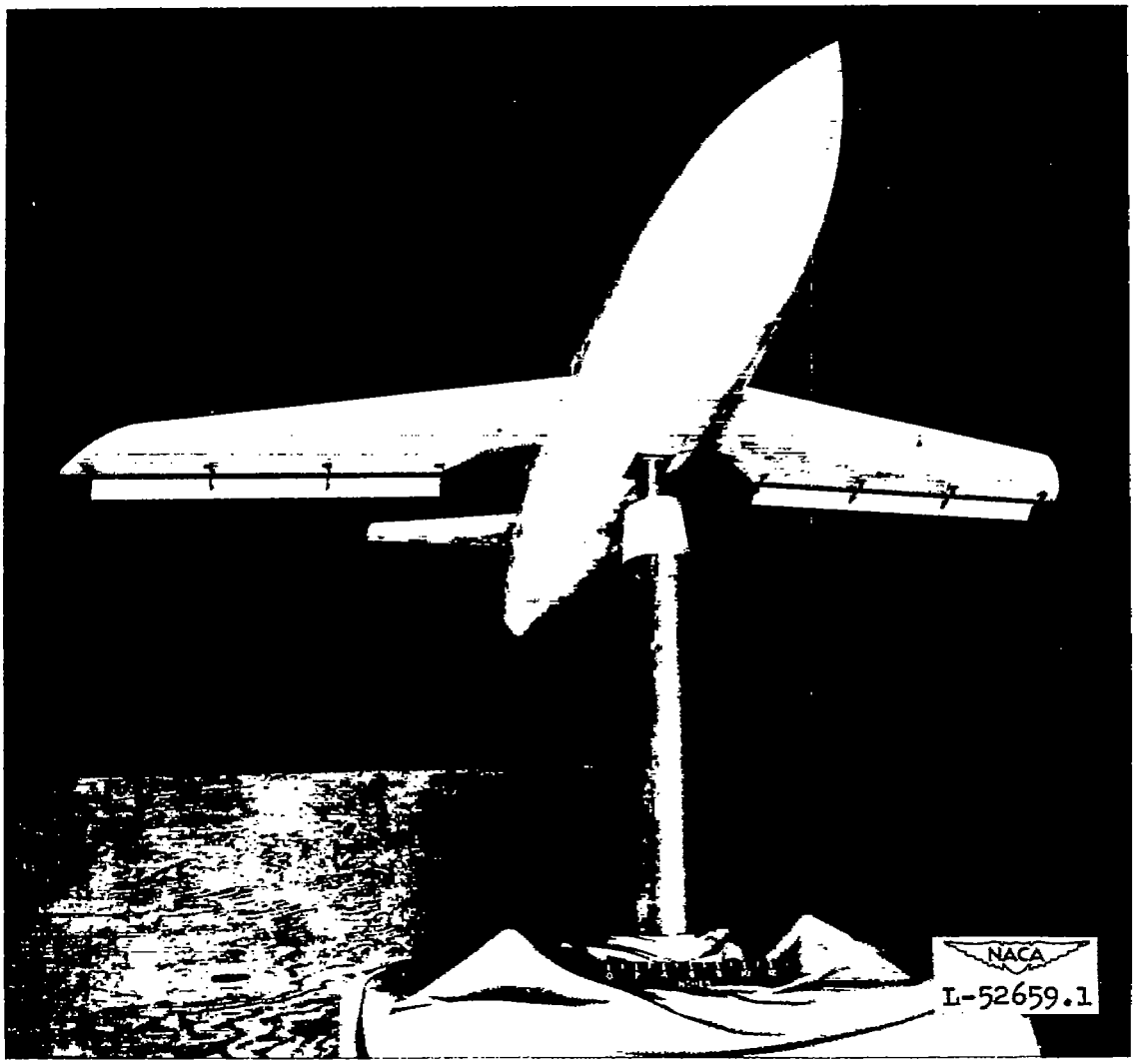

(a) Front view.

Figure 5.- Variable-sweep model mounted on single-support strut with faired cutout and external airfoil flaps. $\Lambda = 15^{\circ}$.

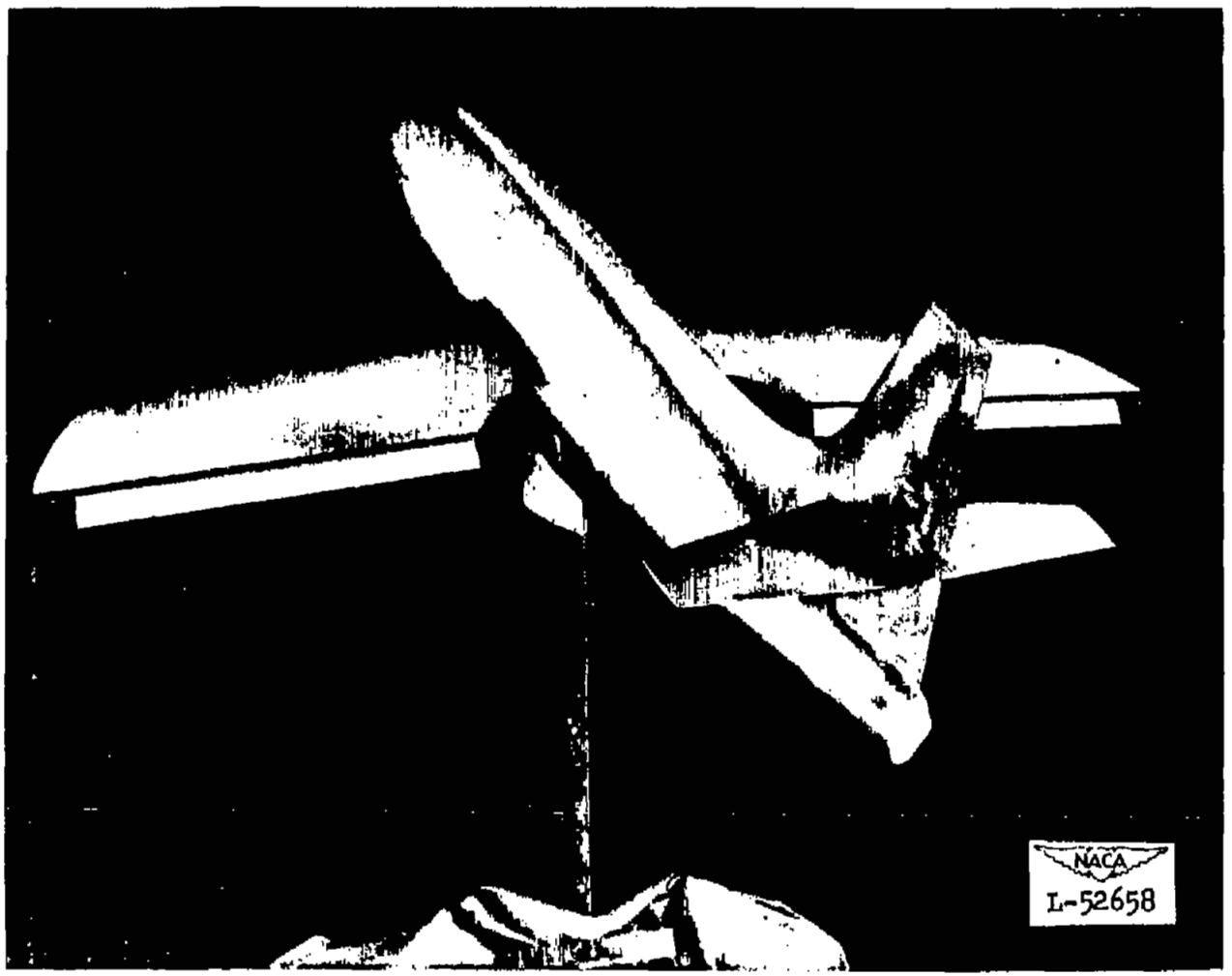

(b) Rear view.

Figure 5.- Concluded.

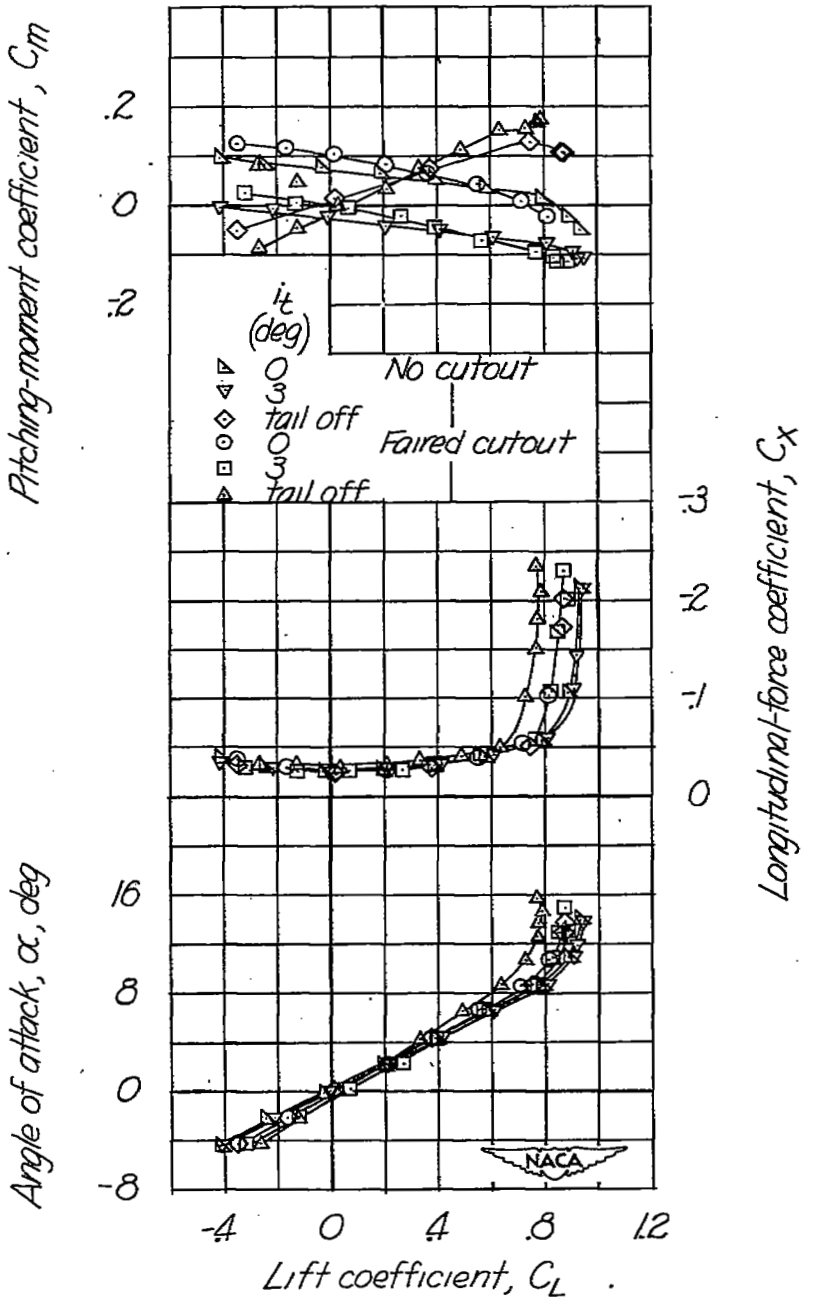

Figure 6.— Aerodynamic characteristics of a variable-sweep model with and without faired wing cutout. $\Lambda = 0°$.

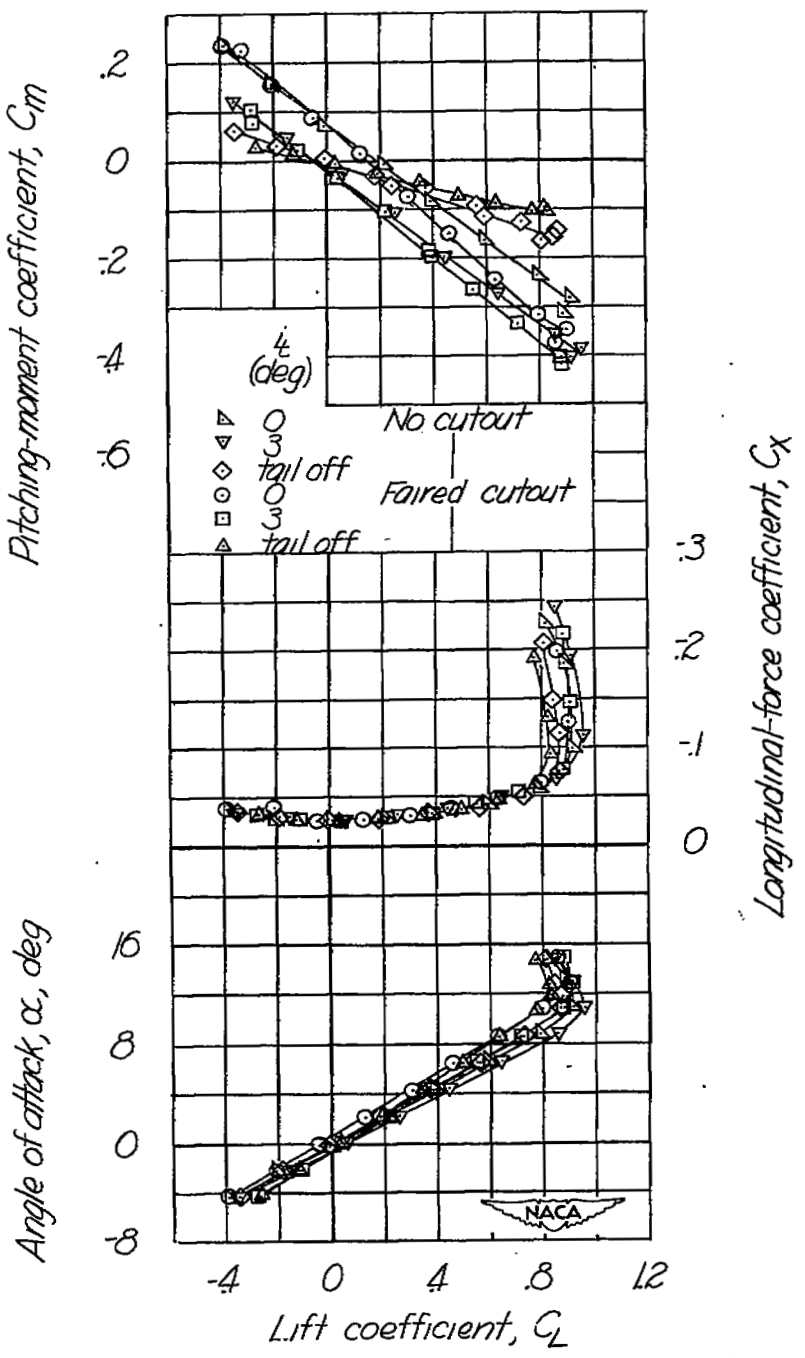

(a) Basic tail position.

Figure 7.– Aerodynamic characteristics of a variable-sweep model with and without wing cutouts. $\Lambda = 15°$.

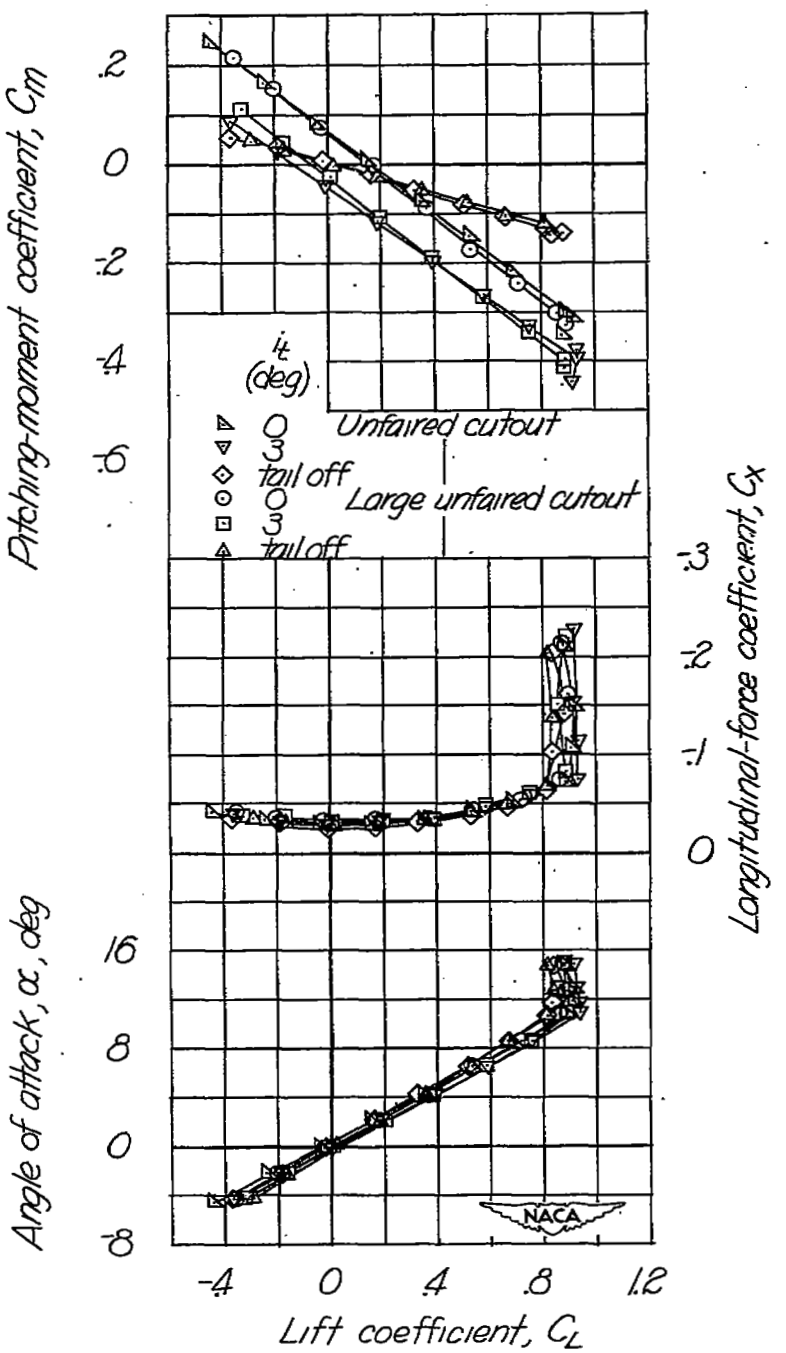

(a) Concluded.

Figure 7.– Continued.

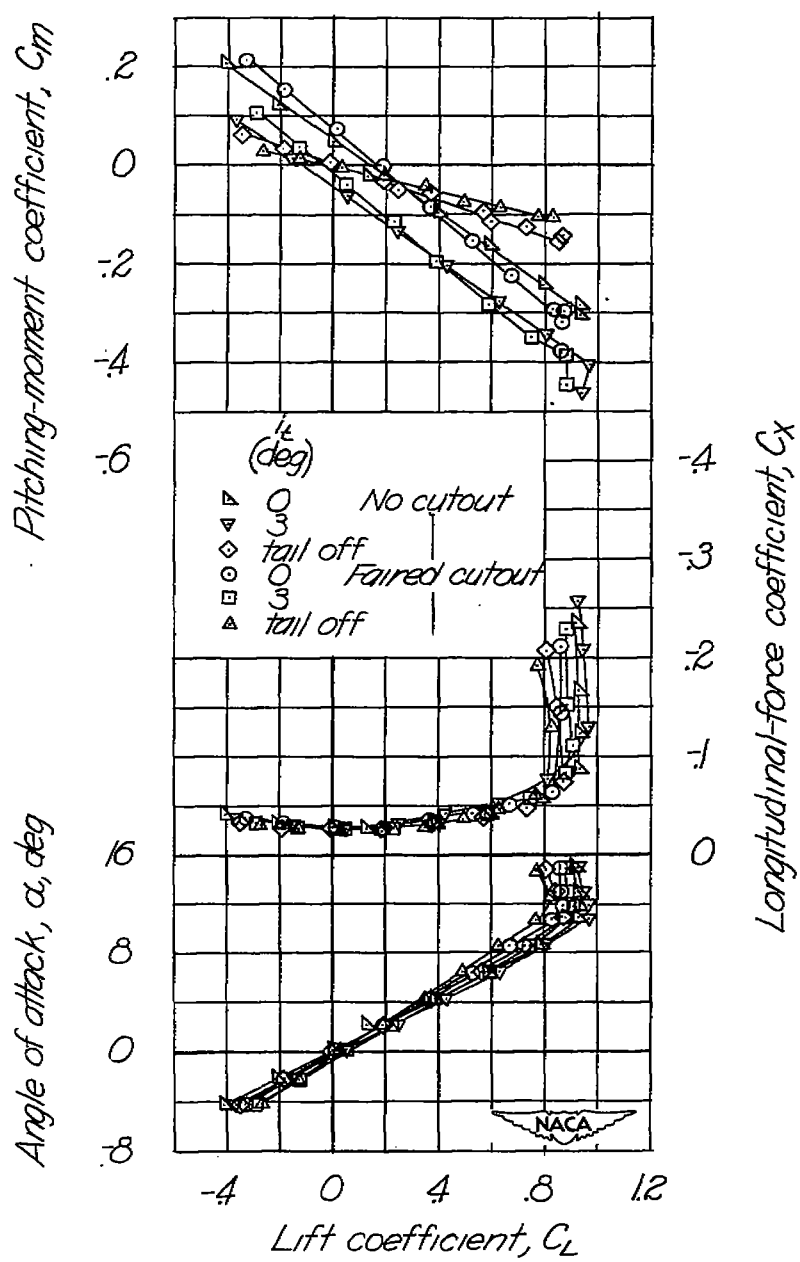

(b) Alternate tail position.

Figure 7.- Continued.

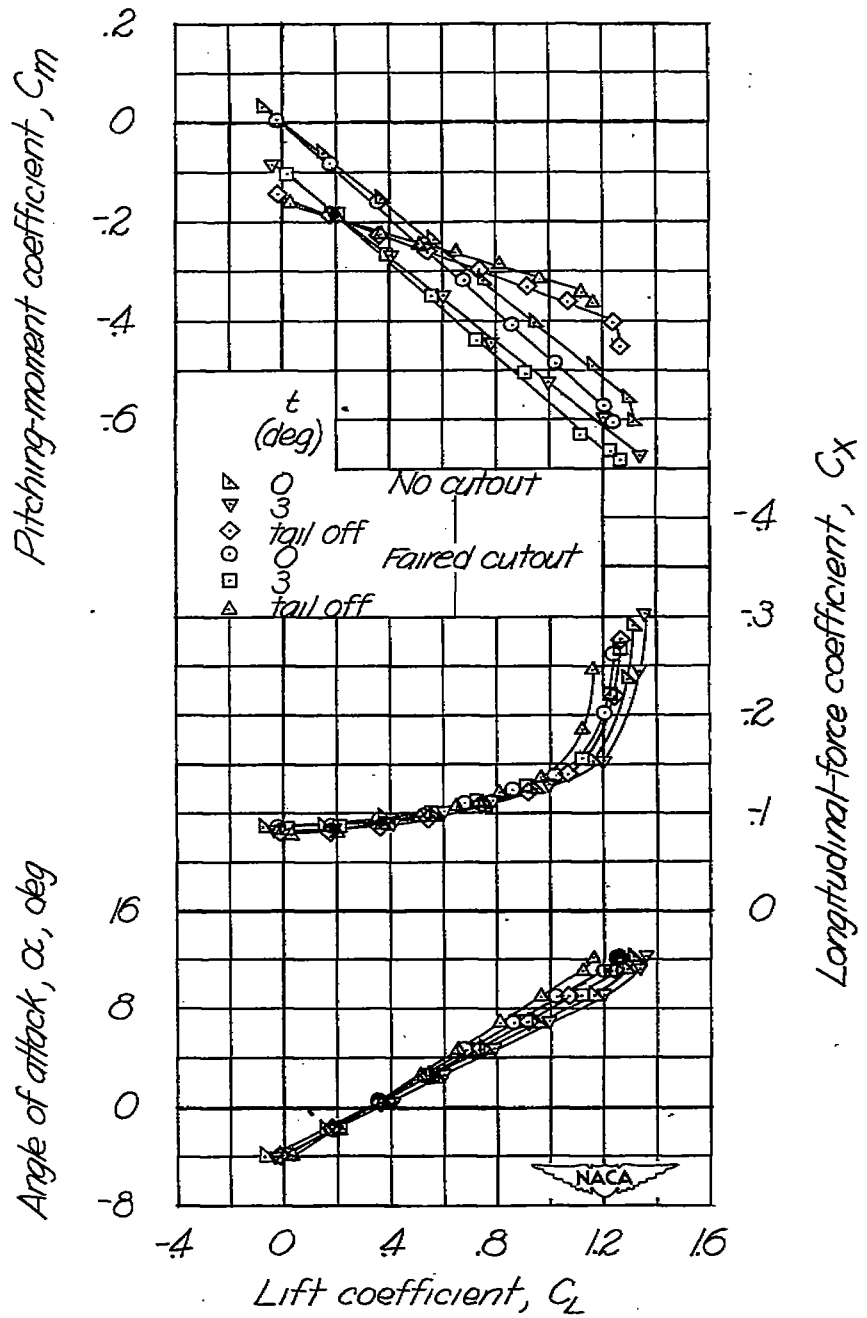

(c) External airfoil flaps.

Figure 7.– Continued.

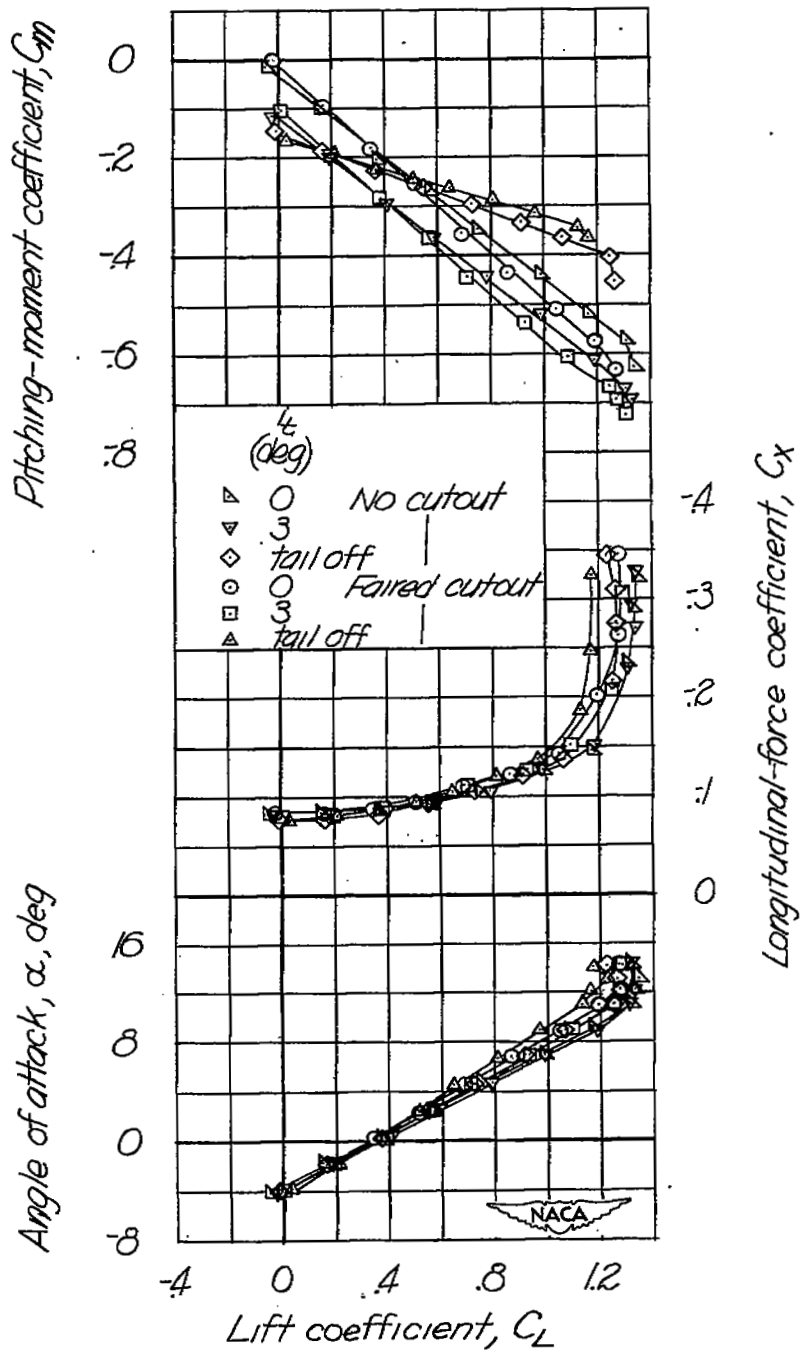

(d) External airfoil flaps, alternate tail position.

Figure 7.– Continued.

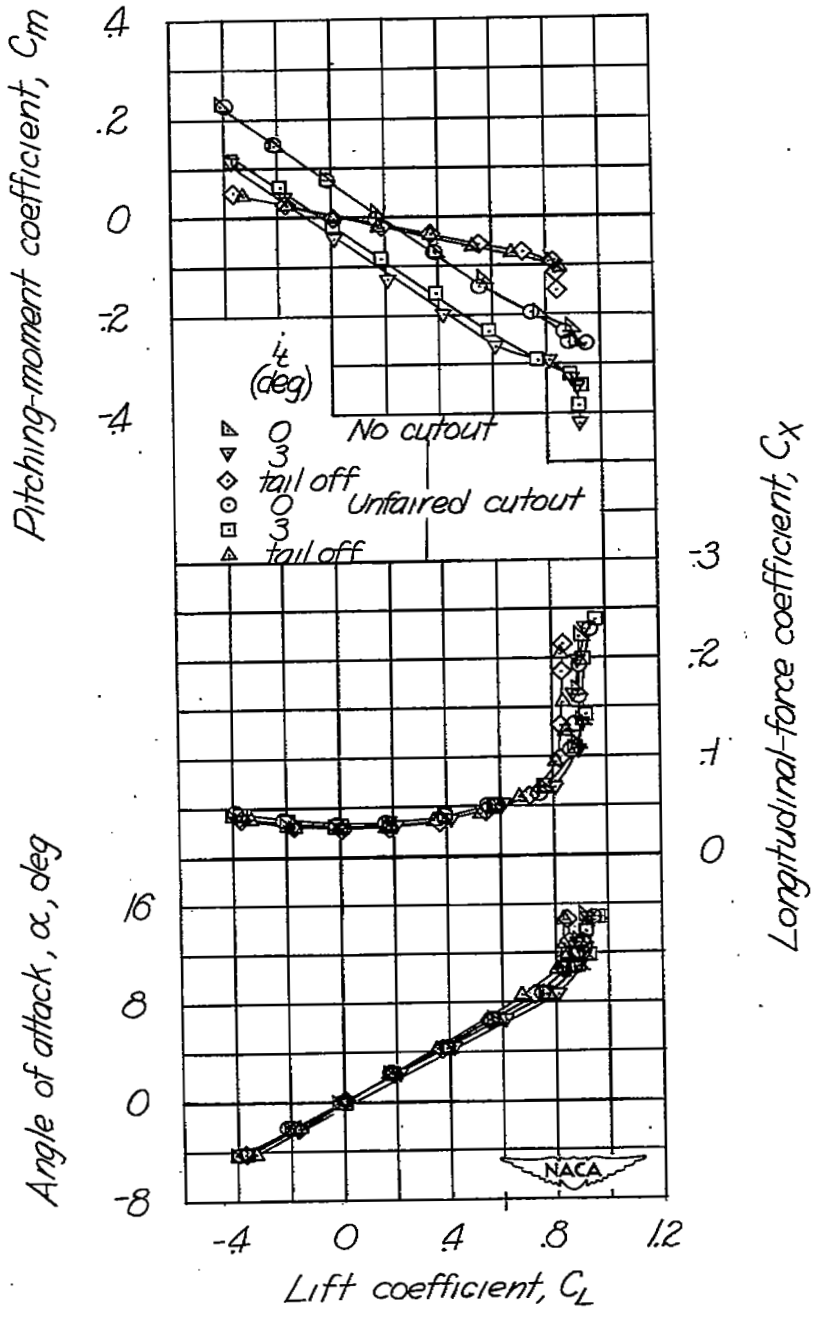

(e) Sharp-leading-edge wing section.

Figure 7.- Continued.

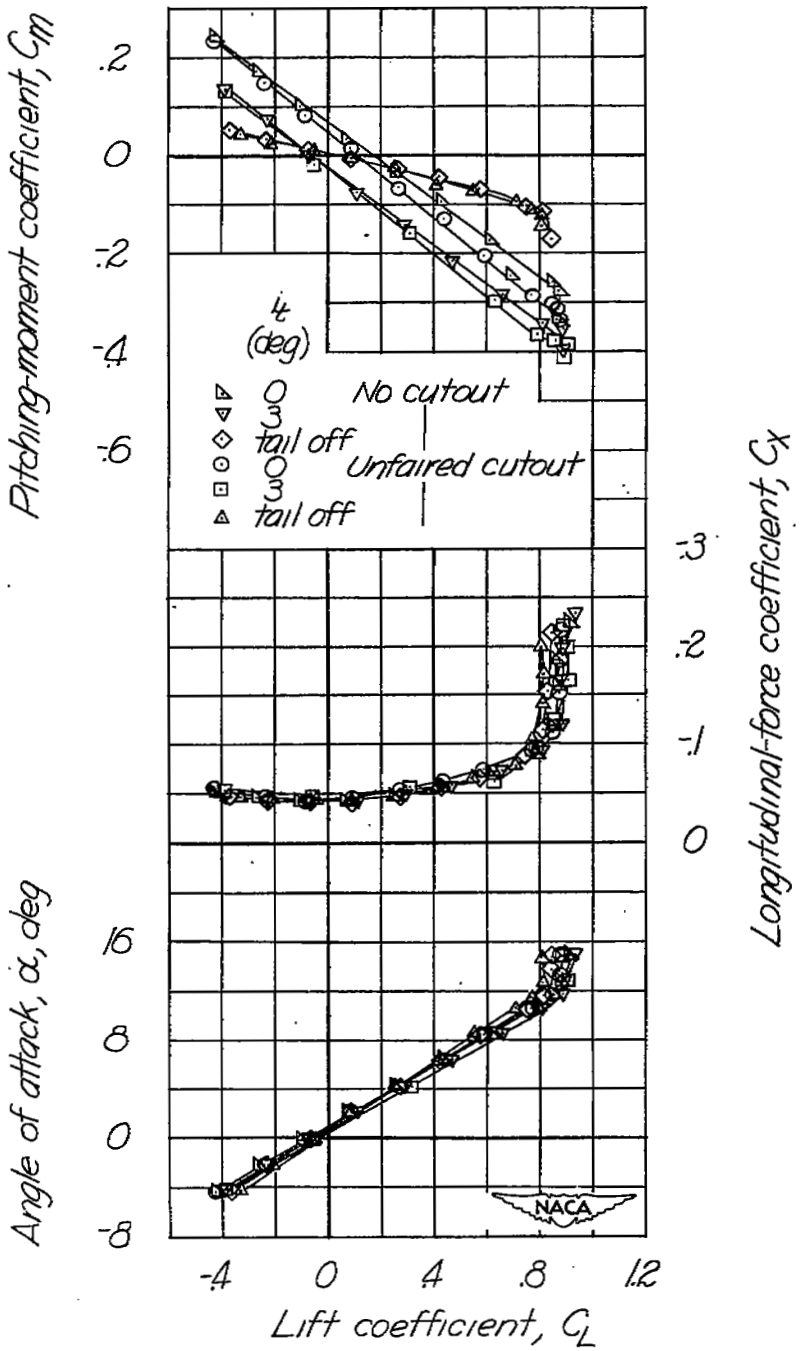

(f) Wing vane.

Figure 7.– Concluded.

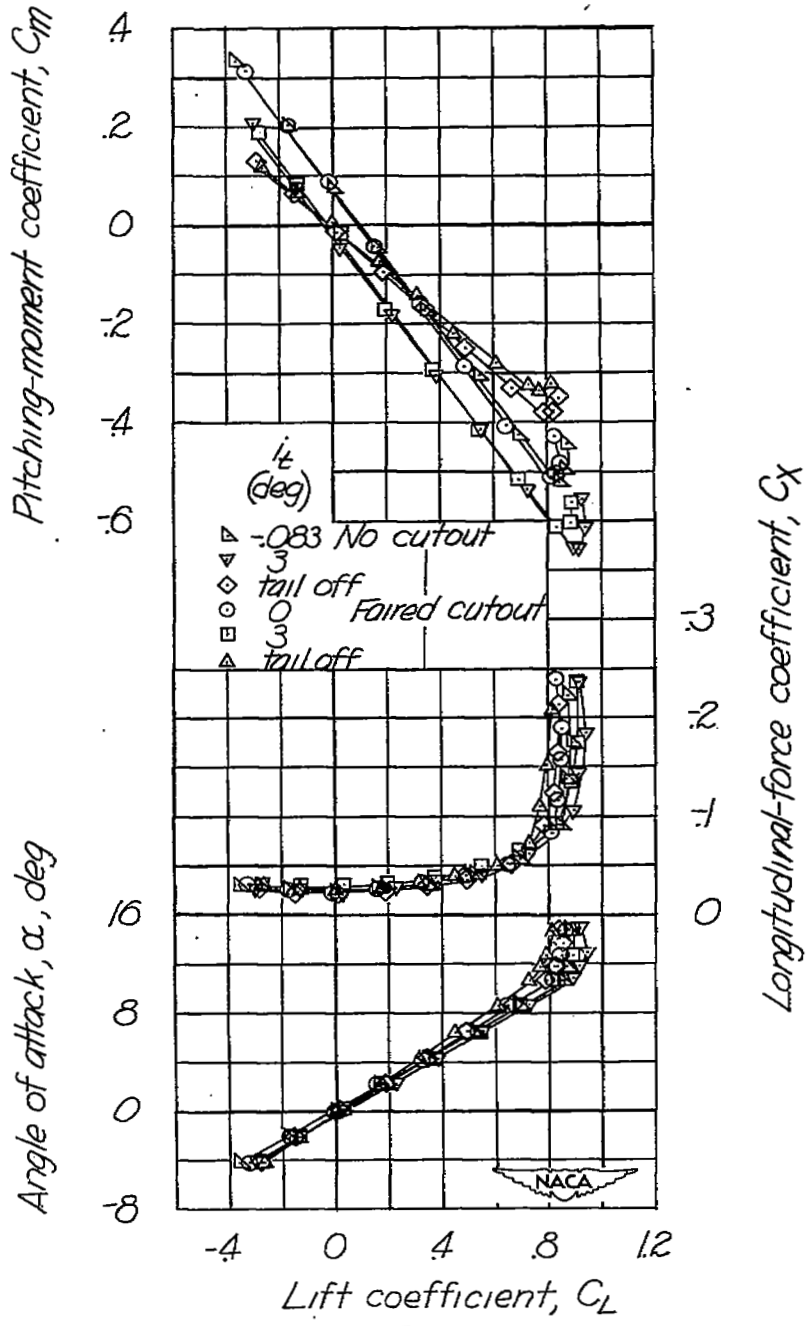

Figure 8.— Aerodynamic characteristics of a variable-sweep model with and without faired wing cutout. $\Lambda = 30°$.

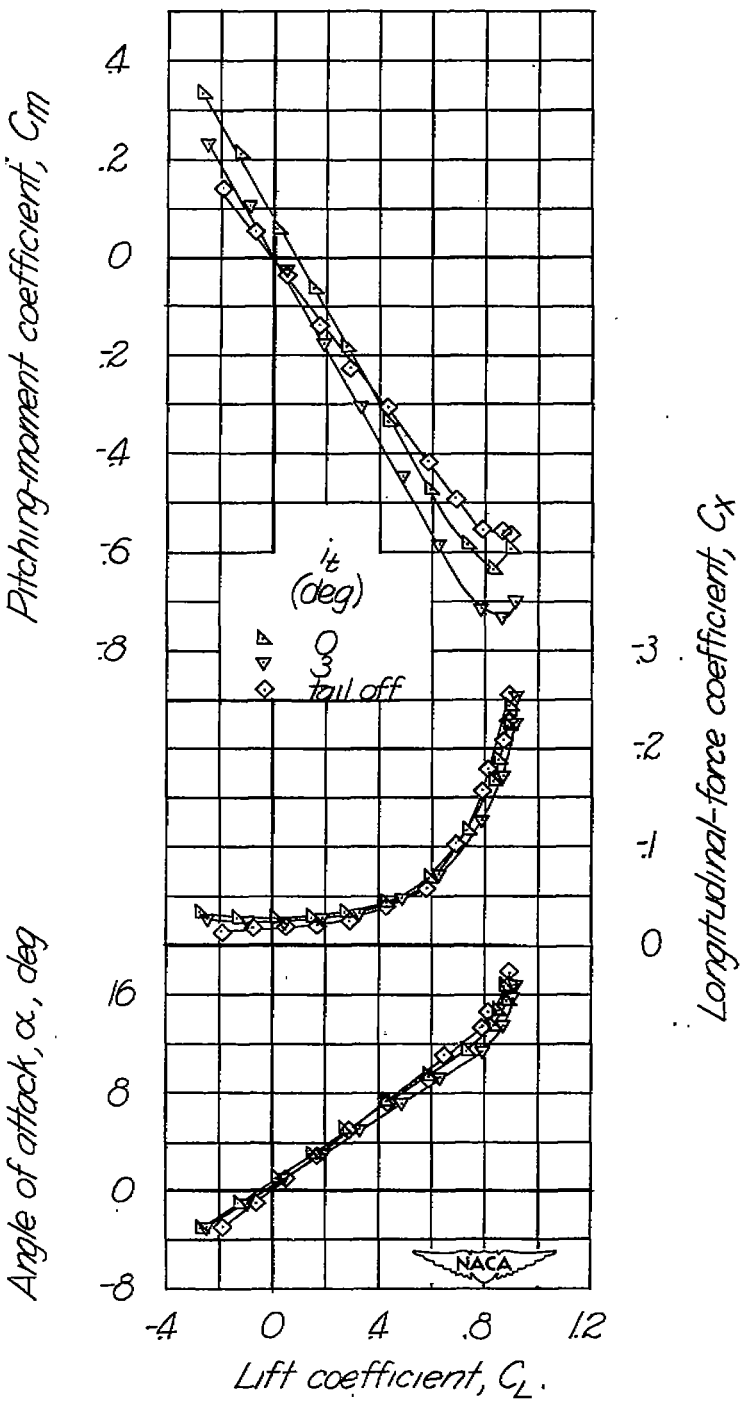

(a) Basic tail position.

Figure 9.– Aerodynamic characteristics of a variable sweep model with two horizontal-tail positions. $\Lambda = 45°$.

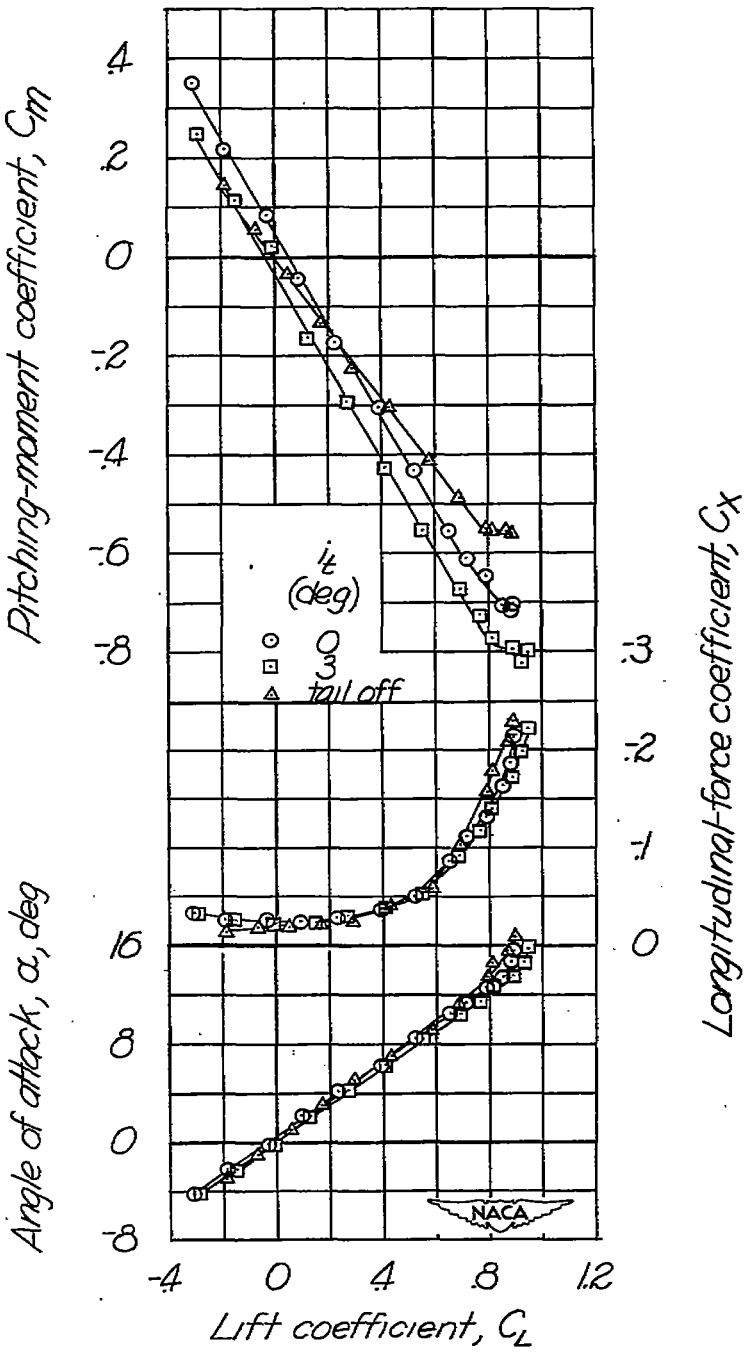

(b) Alternate tail position.

Figure 9.- Concluded.

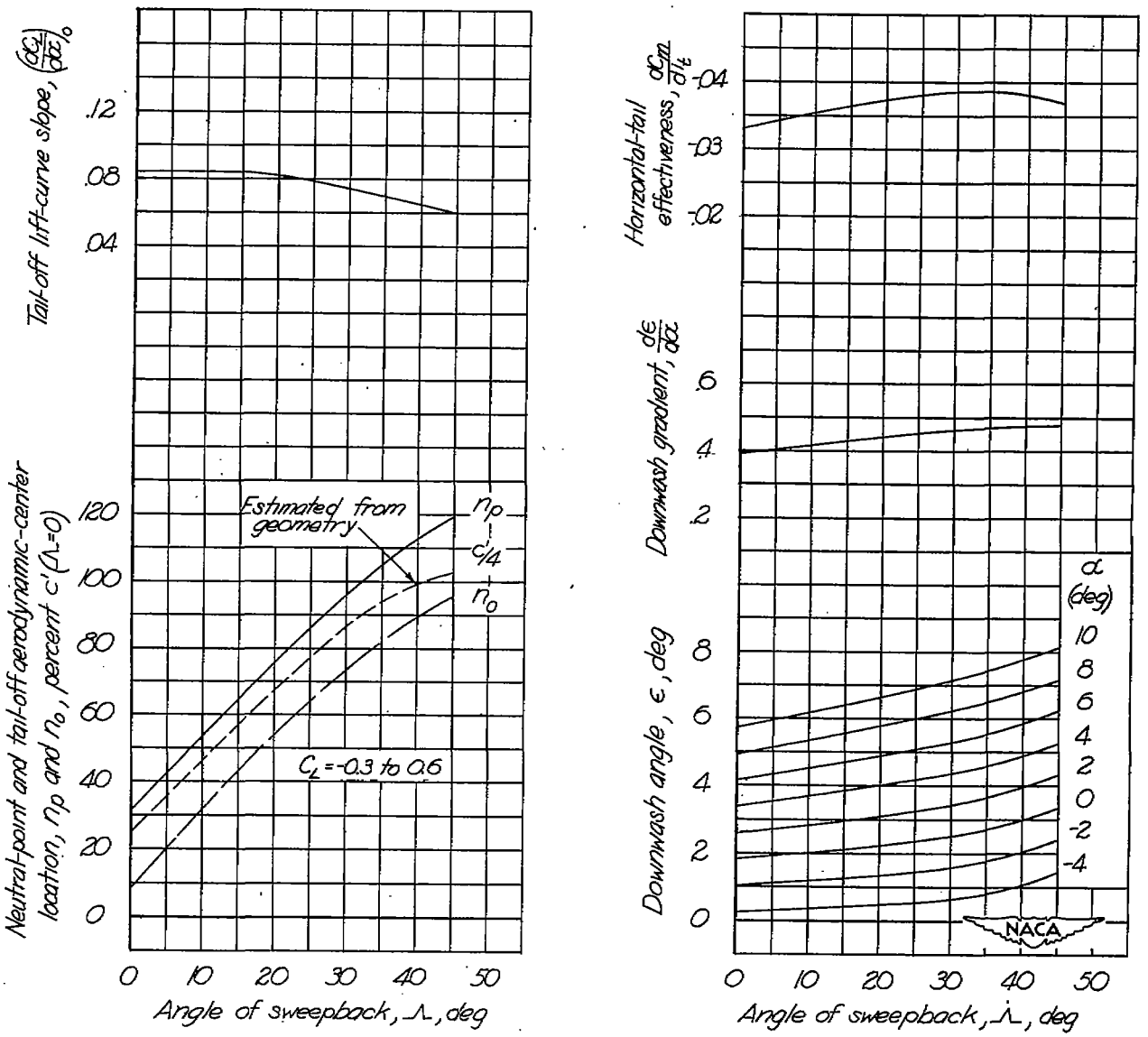

Figure 10.– Variation of longitudinal–stability parameters with angle of sweepback for a variable–sweep model. Basic tail position; wing without cutout.

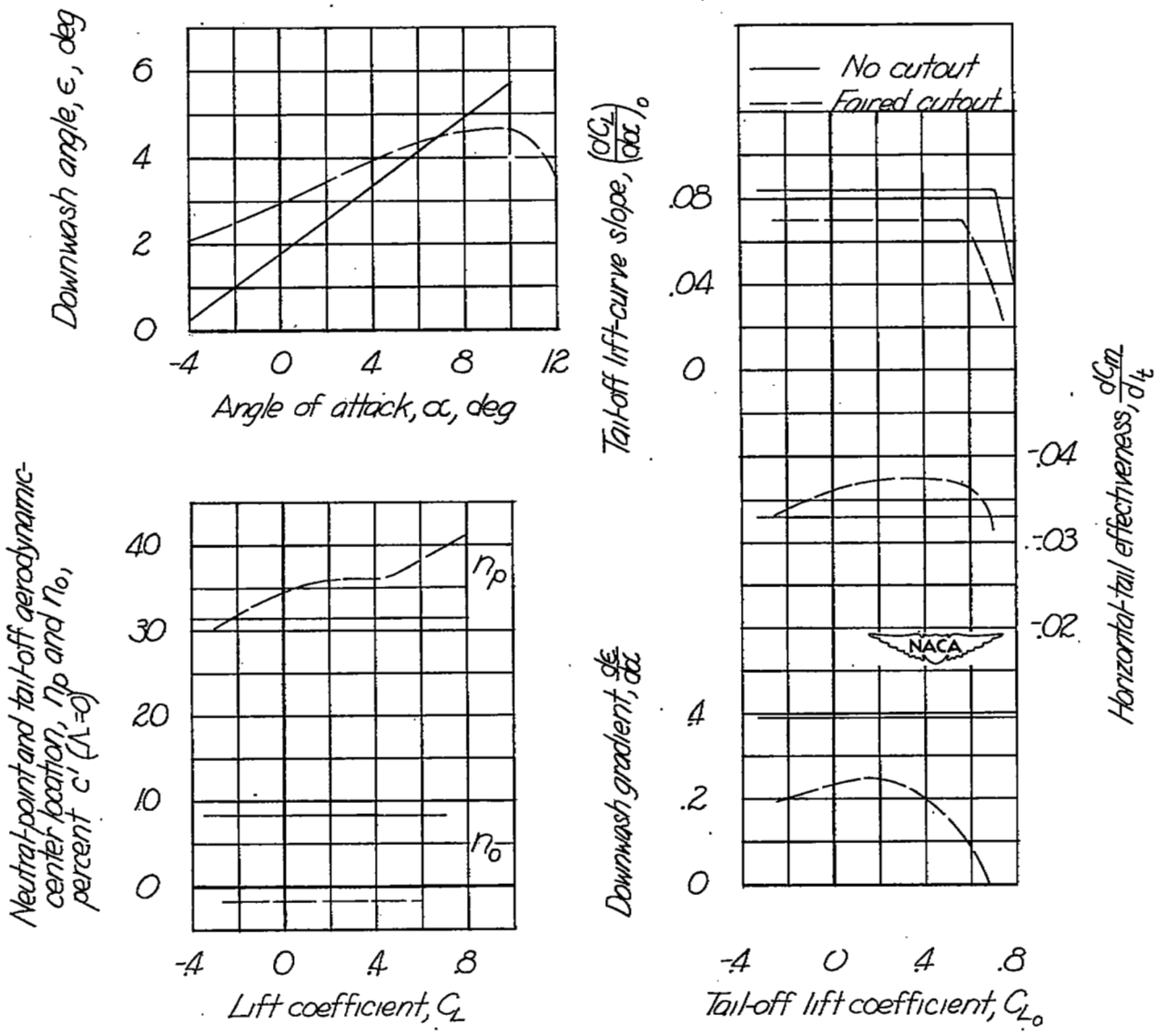

Figure 11.– Longitudinal–stability parameters of a variable–sweep model with and without faired wing cutout. $\Lambda = 0^\circ$.

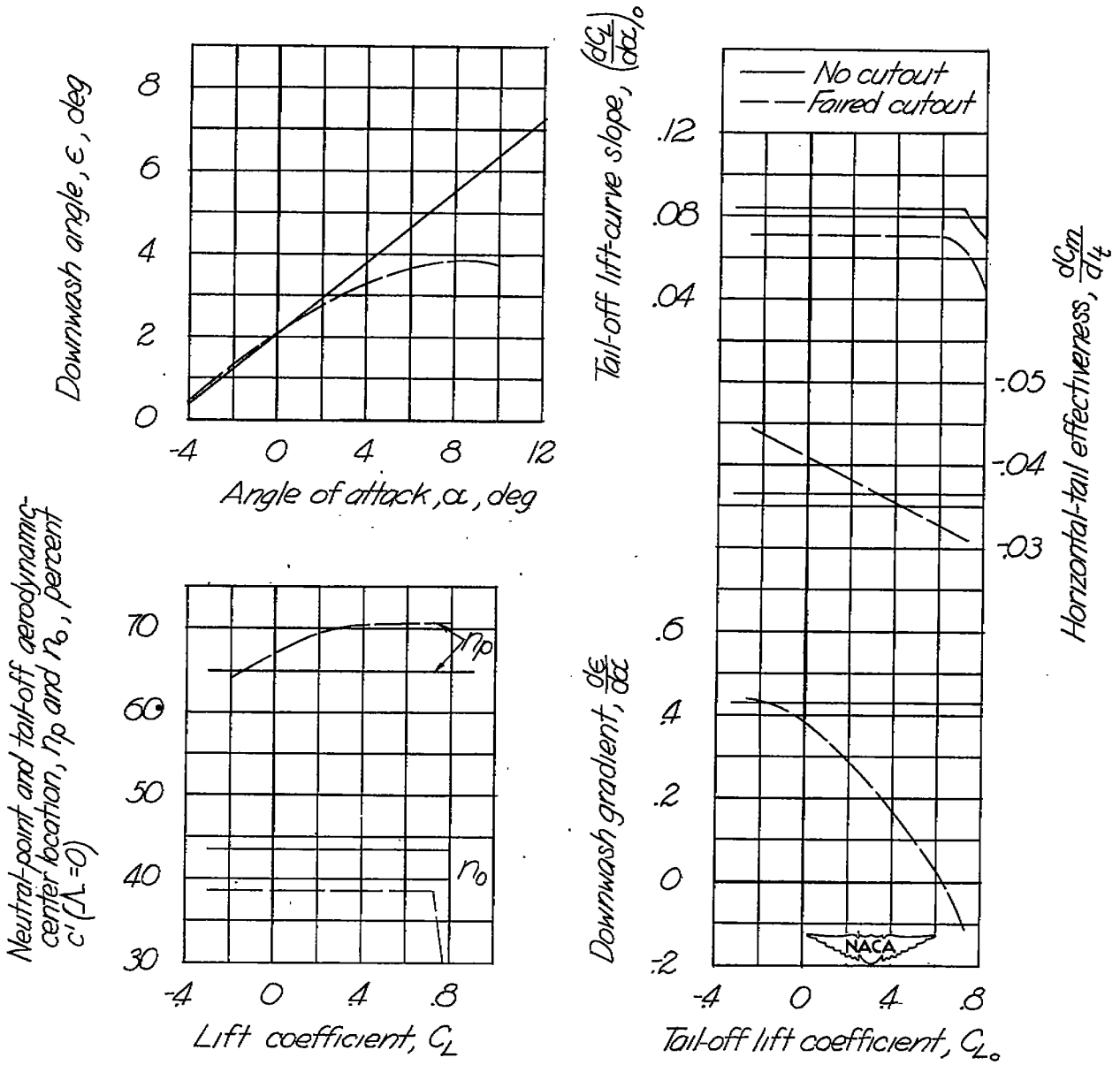

(a) Basic tail position.

Figure 12.– Longitudinal–stability parameters of a variable–sweep model with and without wing cutouts. $\Lambda = 15°$.

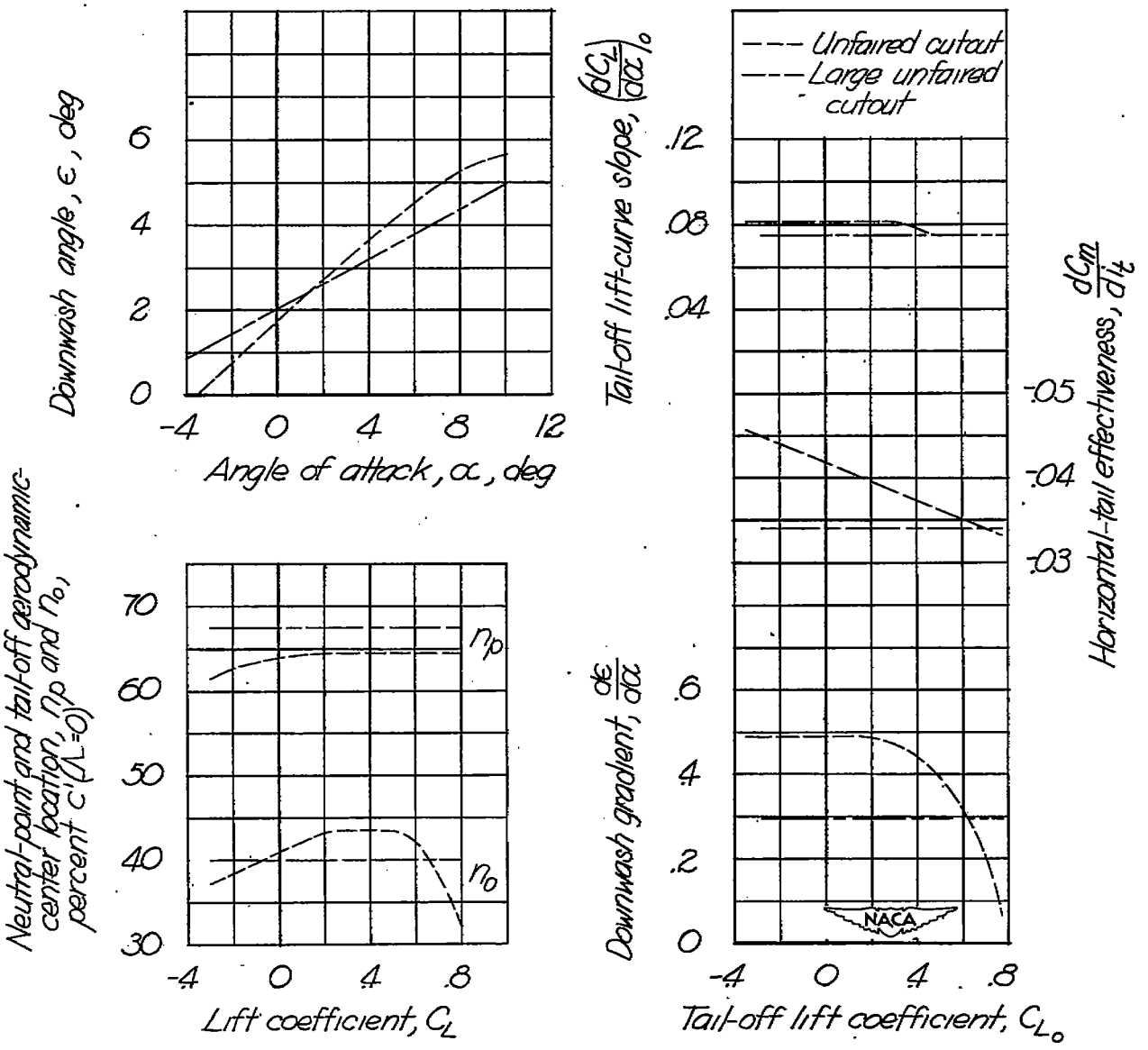

(a) Concluded.

Figure 12.– Continued.

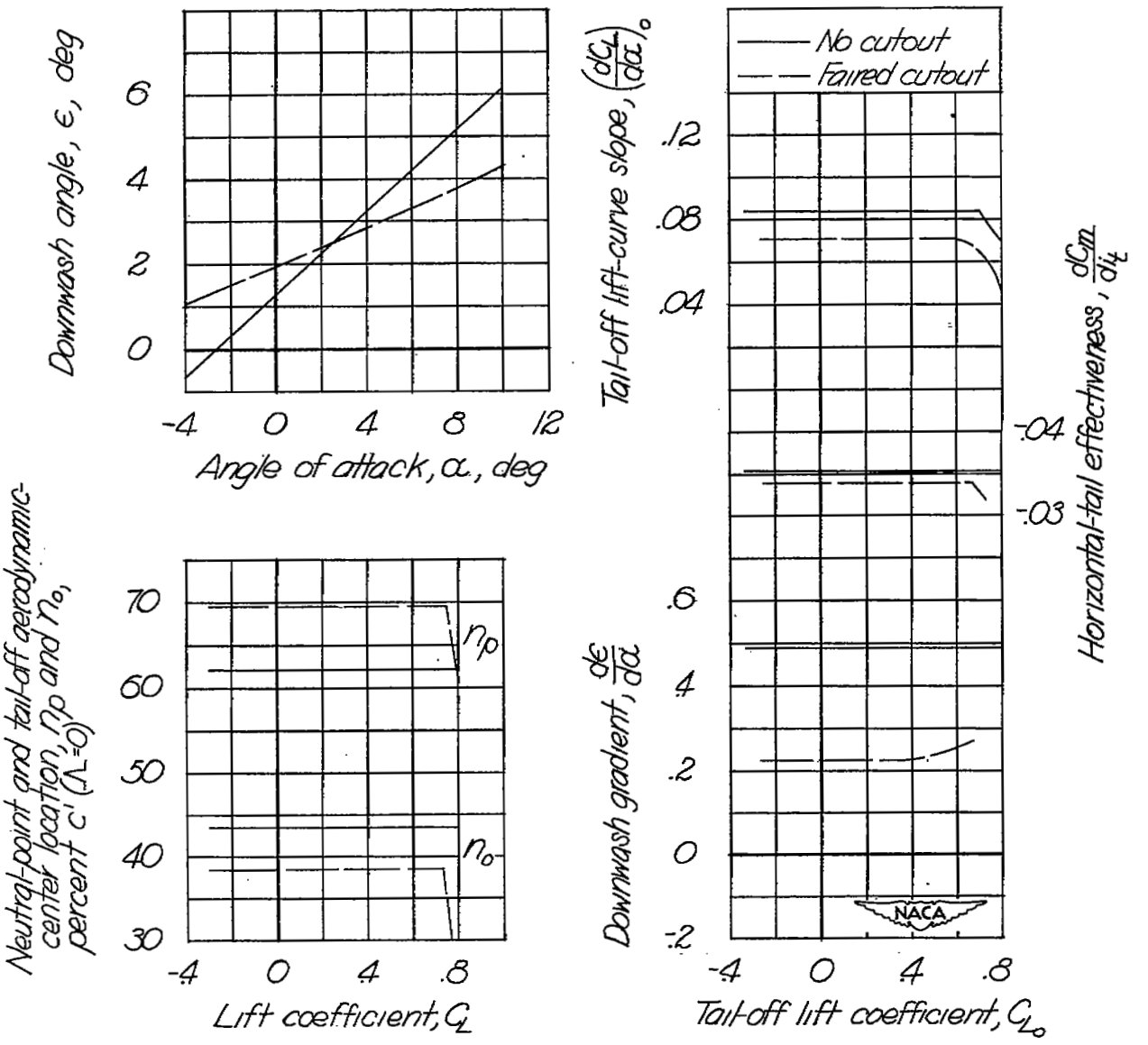

(b) Alternate tail position.

Figure 12.– Continued.

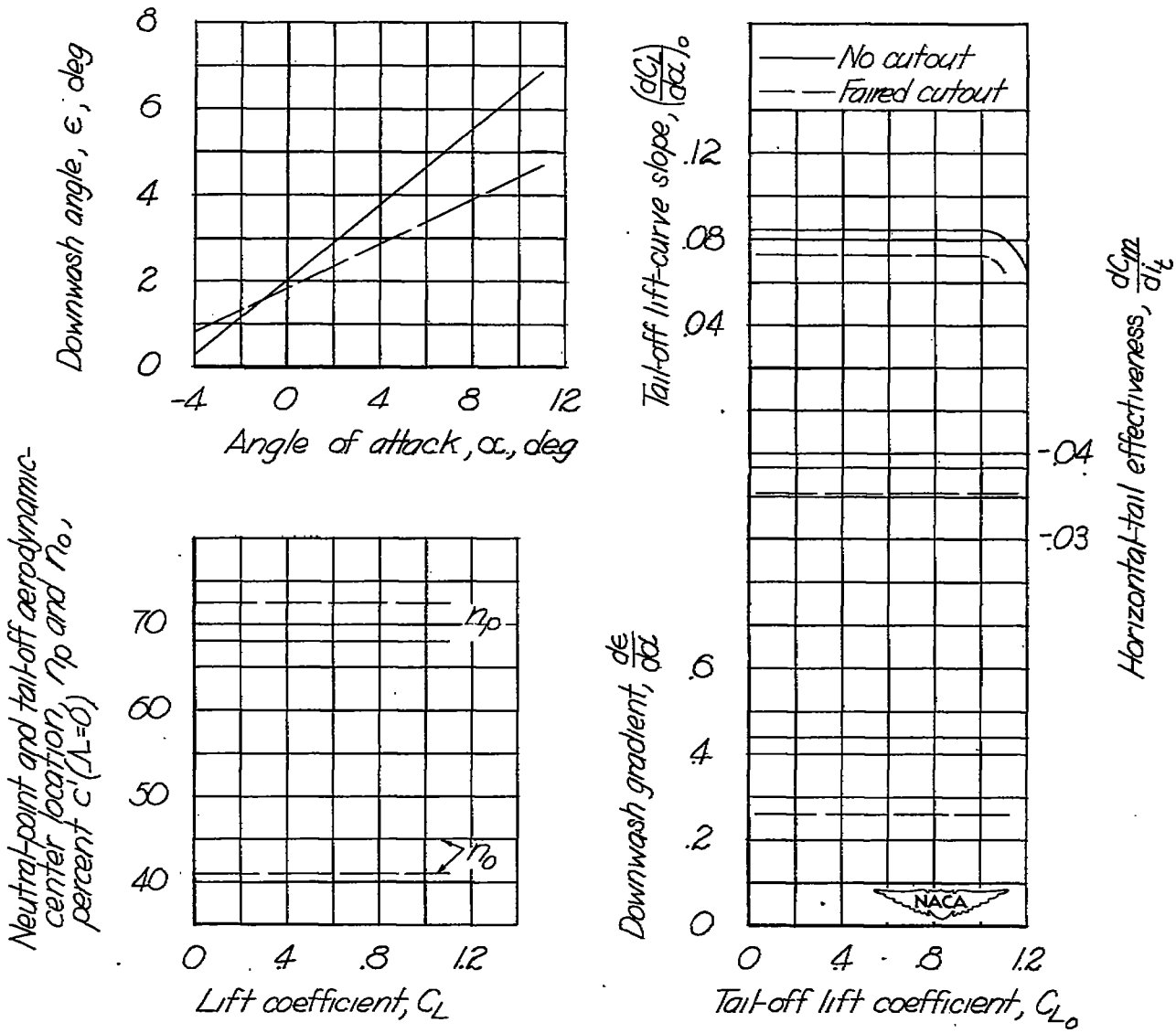

(c) External airfoil flaps.

Figure 12.- Continued.

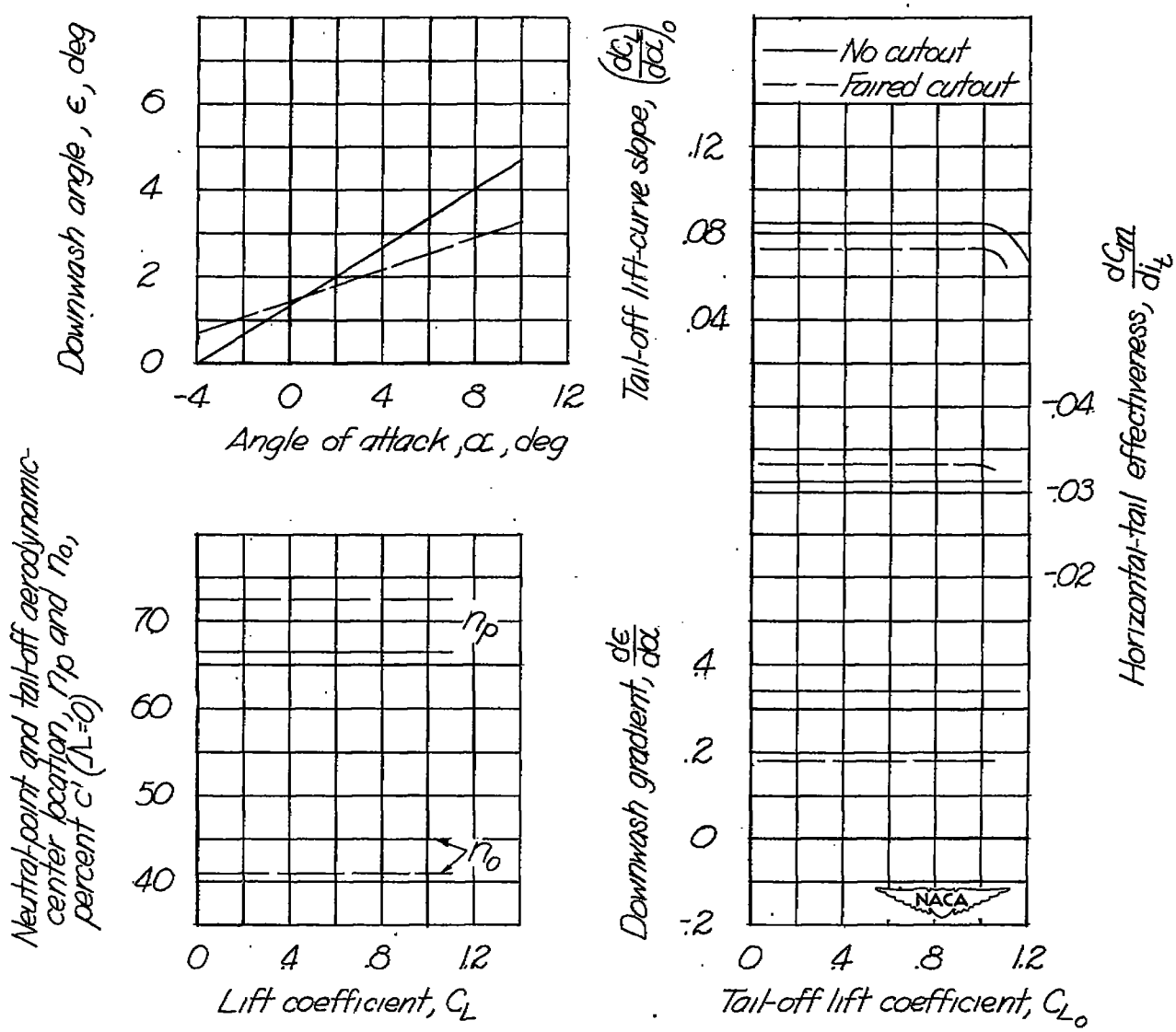

(d) External airfoil flaps, alternate tail position.

Figure 12.– Continued.

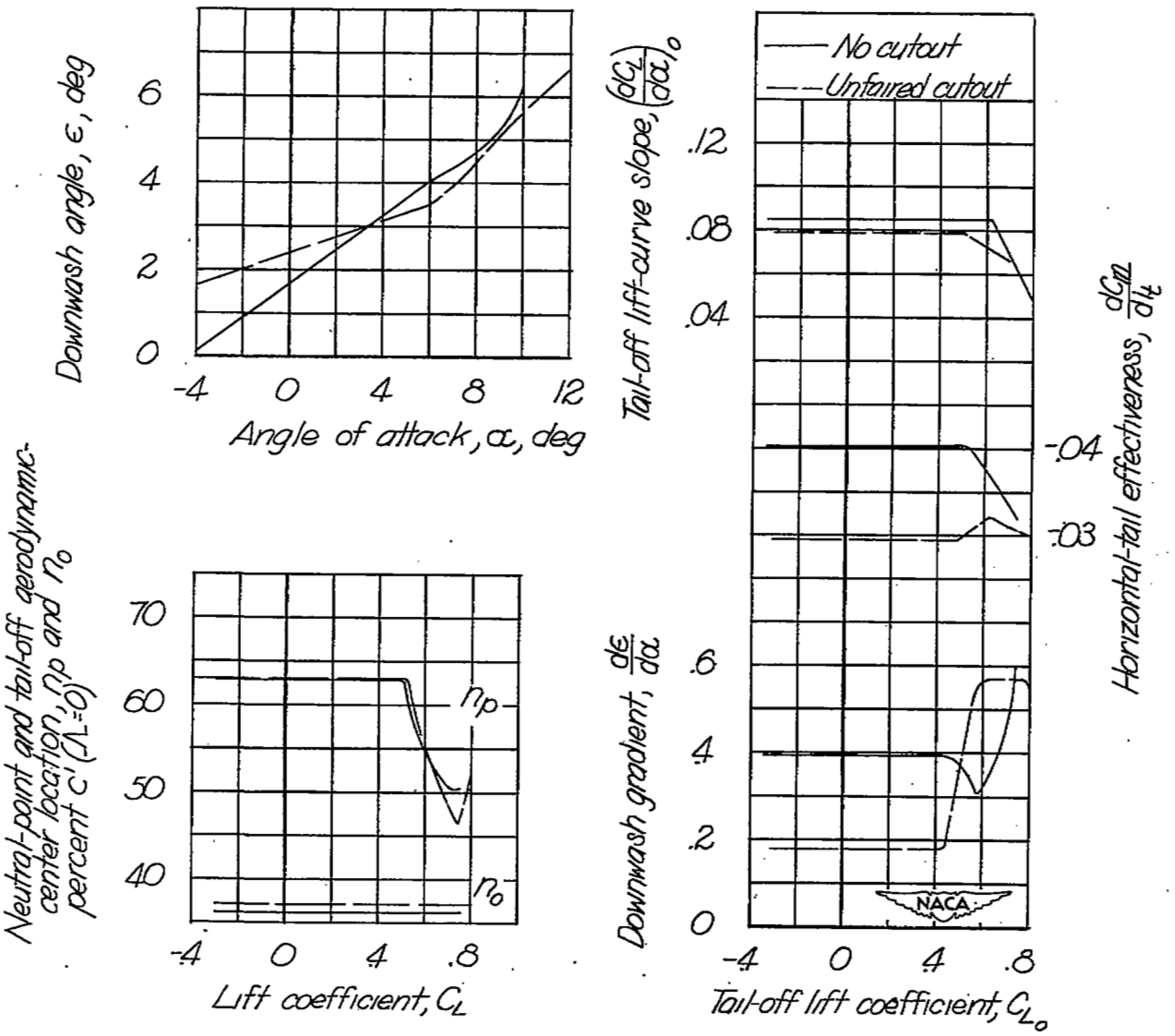

(e) Sharp-leading-edge wing section

Figure 12.— Continued.

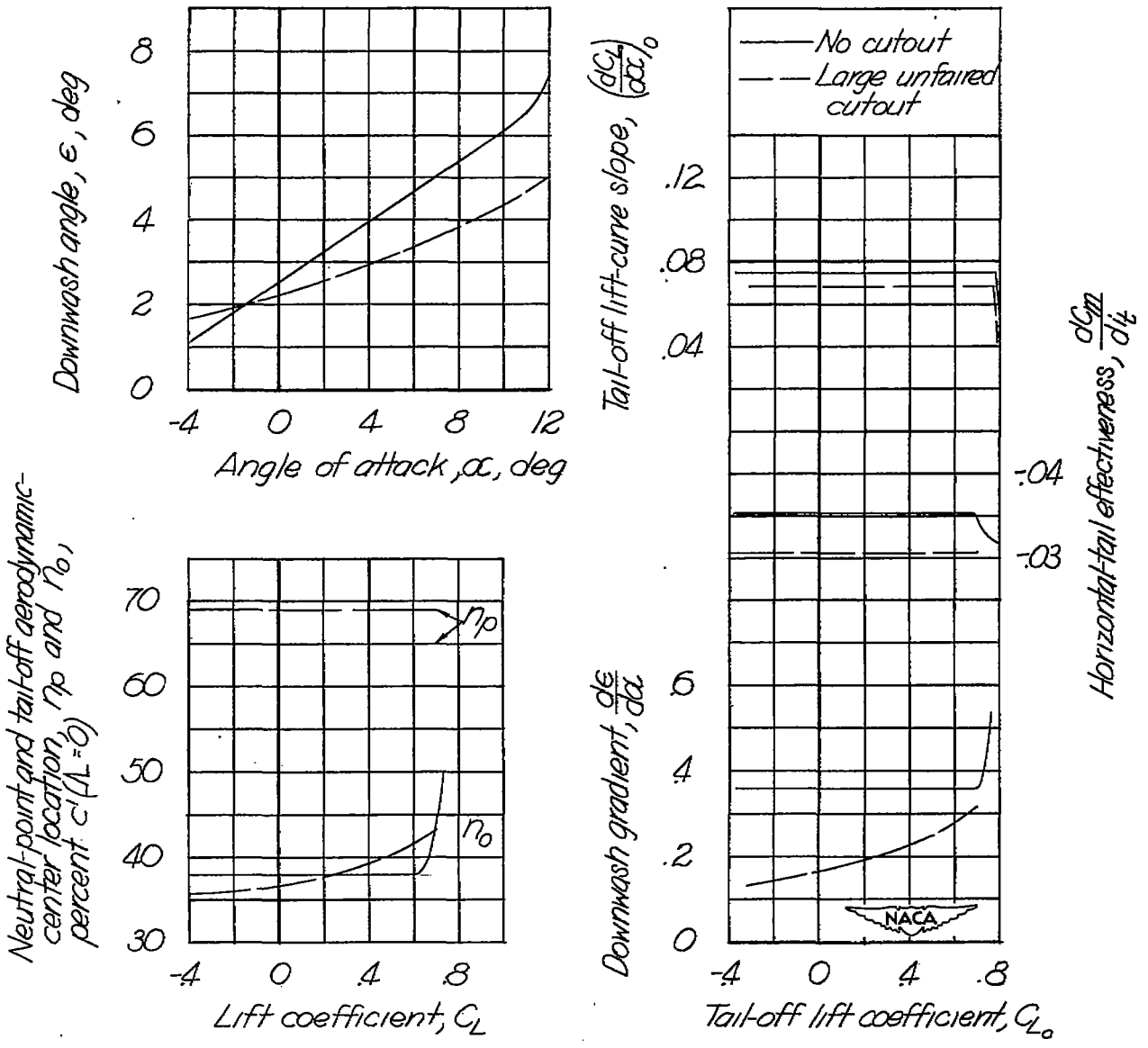

(f) Wing vane.

Figure 12.– Concluded.

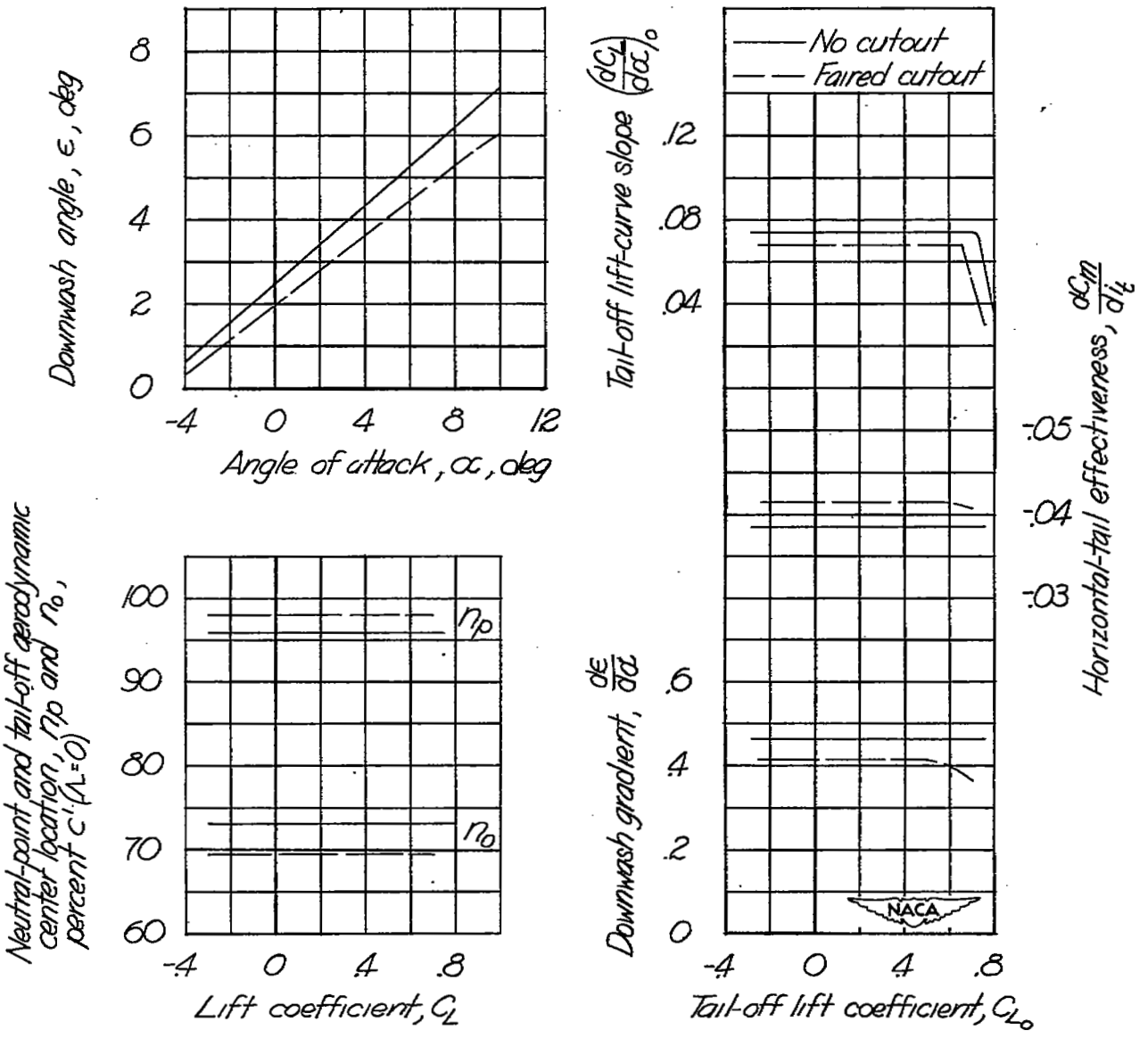

Figure 13.– Longitudinal–stability parameters of a variable–sweep model with and without faired wing cutout. $\Lambda = 30°$.

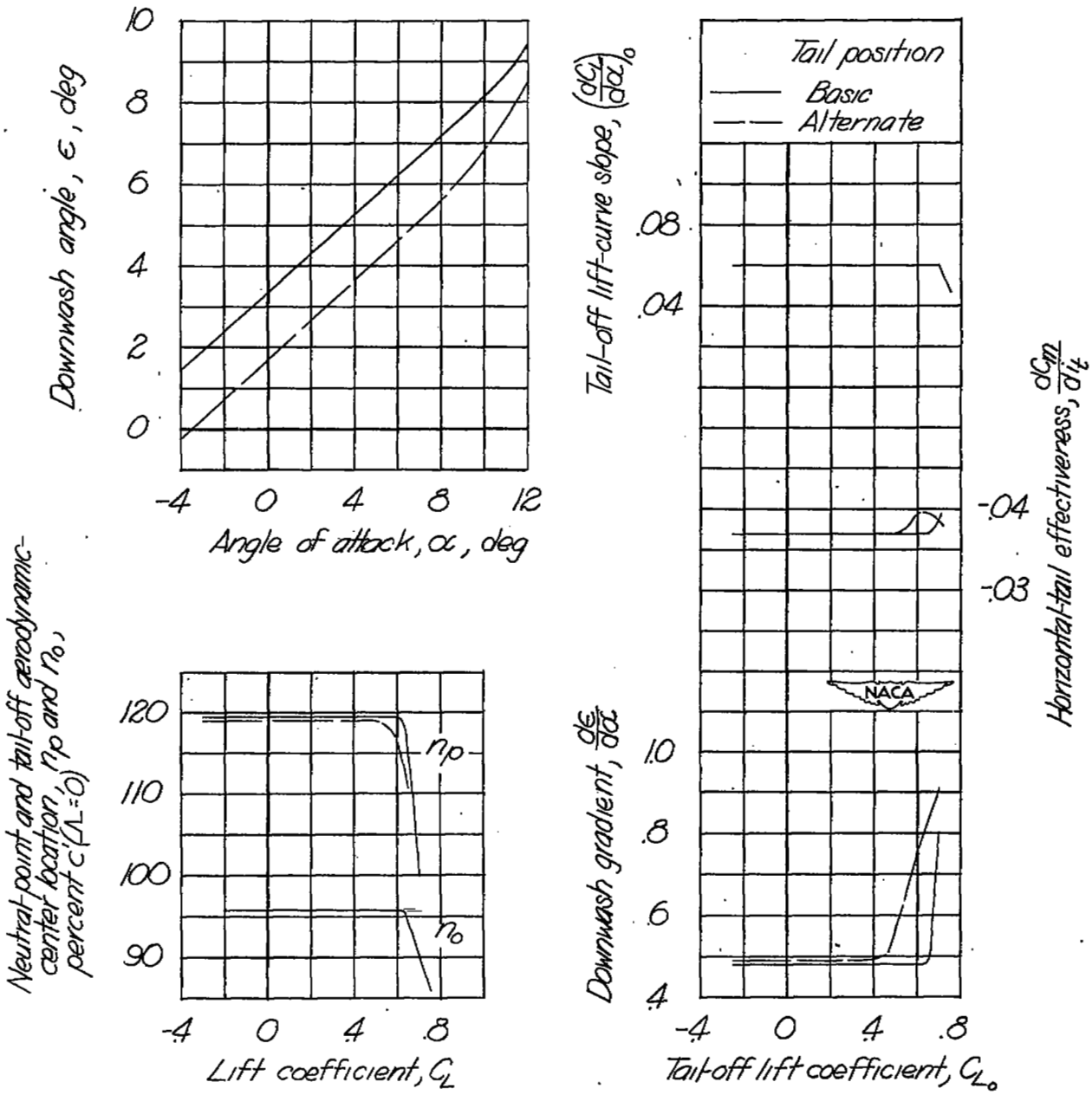

Figure 14.- Longitudinal-stability parameters of a variable-sweep model with two horizontal-tail positions. $\Lambda = 45^\circ$.

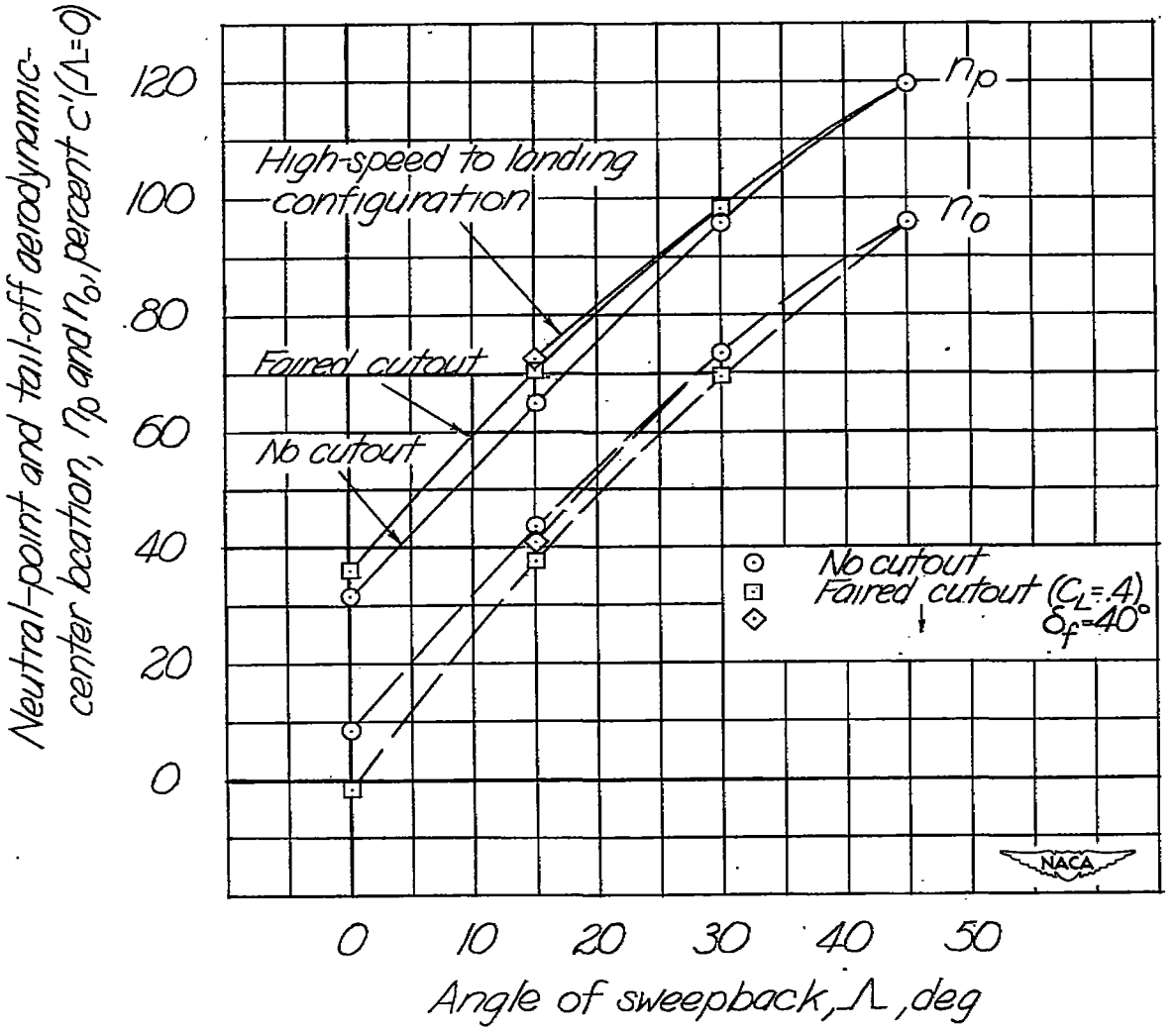

Figure 15.– Variation of longitudinal stability with sweepback and model configuration.